Johannes Wiener

Synthesis and Characterization of Thiol-yne and Thiol-yne-methacrylate Derived Photo-curable Resins

Master Thesis

Montanuniversität Leoben

Chair of Chemistry of Polymeric Materials

Leoben, June 2017

Supervisor:

Assoc. Prof. Dipl.-Ing. Dr. Thomas Grießer

ABSTRACT

The subject of the present thesis is the synthesis of alkyne monomers and the characterization of their photoreactive properties. The novel monomers could serve as component for future thiol-yne and thiol-yne-methacrylate based formulations for UV-based 3D-printing applications.

First, a commercial bifunctional acrylate was successfully converted into a tetrafunctional alkyne by utilizing the Michael addition reaction. In addition to that, two hybrid monomers were created by functionalizing Hydroxyethyl methacrylate with two different alkyne moieties. These hybrid monomers were used as part of a thiol-yne-methacrylate formulation to explore the unique reaction kinetics of ternary systems.

The reaction rate and monomer conversion of various formulations containing the novel monomers were investigated using photo-differential scanning calorimetry (DSC) and real-time Fourier transform infrared spectroscopy (FTIR). The impact of stoichiometry was demonstrated through the comparison of stoichiometric and non-stoichiometric systems. A commercial methacrylate was investigated in the same way so the results could be compared.

The photopolymers of resins containing the novel monomers were tested by dynamic mechanical analysis (DMA) and their toughness was evaluated by crack tip opening angle (CTOA) measurements. A commercial acrylate was investigated in the same way so the results could be compared.

The binary thiol-yne system exhibited good reaction rate as well as high monomer conversion. The ternary systems containing the hybrid monomers showed very good conversions despite the presence of methacrylate. The initially slow reaction rate could be significantly improved by adding Urethane dimethacrylate (UDMA) without influencing monomer conversions.

The photocured thiol-yne formulation provided the highest storage modulus and glass transition temperature (T_G) of the investigated novel resins. Although the T_G of a comparable acrylate could not be reached, a higher storage modulus could be achieved.

In addition, the thiol-yne based formulation proved to have tougher material behavior than a comparable acrylate, resulting in a larger crack tip opening angle.

The benefits of the synthesized monomers include high monomer conversion, tunable reaction rate and advantageous mechanical performance. In conclusion, the novel

compounds represent a suitable substitution and/or valuable supplement for commercial (meth)acrylate systems for UV-based 3D-printing applications.

KURZFASSUNG

Das Thema dieser Arbeit ist die Synthese von Alkin-Monomeren und die Charakterisierung ihrer photoreaktiven Eigenschaften. Die neuartigen Monomere können als Bestandteil für zukünftige Thiol-In und Thiol-In-Methacrylate Formulierungen für UV-basierte 3D-Druck Anwendungen dienen.

Zuerst wurde ein handelsübliches bifunktionelles Acrylat durch die Michael Additionsreaktion erfolgreich in ein tetrafunktionelles Alkin umgewandelt. Außerdem wurden zwei Hybridmonomere hergestellt, indem Hydroxyethylmethacrylat mit zwei verschiedenen Alkingruppen funktionalisiert wurde. Diese Hybridmonomere wurden als Teil eines Thiol-In-Methacrylat Systems verwendet, um die einzigartige Reaktionskinetik von ternären Systemen zu erforschen.

Die Eigenschaften der drei neuartigen Monomere und deren Photopolymere wurde mit handelsüblichen (Meth)acrylatsystemen verglichen. Die Reaktionsgeschwindigkeit und der Monomerumsatz von verschiedenen Formulierungen, welche die neuartigen Monomere enthielten, wurden mittels dynamischer Photo-Differenzkalorimetrie (Photo-DSC) und real-time Fourier-Transformations-Infrarotspektroskopie untersucht. Der Einfluss der Stöchiometrie wurde aufgezeigt durch den Vergleich von stöchiometrischen und nicht stöchiometrischen Formulierugen. Ein handelsübliches Methacrylat wurde auf dieselbe Weise untersucht, sodass die Ergebnisse verglichen werden konnten.

Die Photopolymere von Formulierungen, welche die neuartigen Monomere enthielten, wurde mittels dynamisch-mechanischer Analyse (DMA) getestet und deren Zähigkeit wurde durch Messungen des Rissspitzenöffnungswinkels (CTOA) bewertet. Ein handelsübliches Acrylat wurde auf dieselbe Weise untersucht, sodass die Ergebnisse verglichen werden konnten.

Das binäre Thiol-In System zeigt sowohl gute Reaktionsgeschwindigkeiten als auch hohe Monomerumsätze. Die ternären Systeme der Hybridmonomere zeigten sehr gute Monomerumsätze trotz der Gegenwart von Methacrylat. Die anfänglich langsame Reaktionsgeschwindigkeit konnte durch den Zusatz von Urethandimethacrylat (UDMA) signifikant erhöht werden ohne die Monomerumsätze zu beeinflussen.

Die Thiol-In basierte Formulierung zeigte den höchsten Speichermodul und die höchste Glasübergangstemperatur unter den neuartigen Verbindungen. Der Speichermodul eines vergleichbaren Acrylats konnte ebenfalls übertroffen werden.

Es konnte gezeigt werden, dass die Thiol-In basierte Formulierung zäheres Materialverhalten aufweist als ein vergleichbares Acrylat, was zu einem größeren Rissspitzenöffnungswinkel führte.

Die Vorteile der neuartigen Monomere beinhalten hohe Monomerumsätze, einstellbare Reaktionsgeschwindigkeiten sowie vorteilhafte mechanische Eigenschaften. Schlussendlich kann gesagt werden, dass die neuartigen Verbindungen einen geeigneten Ersatz und/oder eine wertvolle Ergänzung für handelsübliche (Meth)acrylatsysteme für UV-basierte 3D-Druckanwendungen darstellen.

ACKNOWLEDGEMENT

Statutory Declaration

I hereby declare in lieu of oath, that I wrote this thesis and performed the associated research myself, using only the support indicated in the acknowledgments and literature cited in this volume.

Eidesstattliche Erklärung

Ich erkläre an Eides statt, dass ich diese Arbeit selbstständig verfasst und die damit in Verbindung stehende Forschungsarbeit selbst durchgeführt habe, wobei ich nur die angegebenen Quellen und Hilfsmittel verwendet habe.

Leoben, June 2017   Johannes Wiener, Bsc

INDEX

1   Motivation and outline

In recent years UV-based 3D printing technologies such as stereolithography has become a growing field of research in biomedical engineering. The fabrication of drilling guides for dental implants or ear-shaped hearing aids is already considered as state of the art. [1], [2] More novel applications such as bone replacement scaffolds are yet to be mastered. In this example of tissue engineering, magnet resonance scan or computer tomography provide the basis for a three-dimensional implant model. [3], [4] The desired shape is customized digitally and a unique CAD model is generated. A patient specific implant with micro-pores ranging from 50-1000 µm to optimize bone ingrowth can be manufactured within hours. [5], [6], [7] With the advance of this novel technique production cost and time are expected to drastically decrease while providing medical devices of previously unknown quality.

A variety of materials, reaching from metals [8], [9] and ceramics [9], [10], [11] to polymers [12], [13], [14] can be processed. Every material class possesses their own unique profile of properties spanning not only physical, chemical and mechanical features, but also process behavior and physiological interactions such as biocompatibility and degradability. [15] Polymers represent the most adaptable class of materials due to the great freedom of design in their molecular structure. A broad spectrum of properties can be realized through tailor-made resin systems that are optimized for their specific field of application. [16], [17]

Commonly used resins for lithographic 3D printing are multifunctional, commercial acrylates and methacrylates, both of which exhibit a chain-growth mechanism. [17] For biomedical applications in particular this circumstance gives rise for three problems:

Firstly, the heterogeneous network structure and internal stresses of chain-growth polymers lead to material brittleness, which is a major drawback for implants and other mechanically demanding applications. [17], [18], [19]

Secondly, the chain-growth mechanism features limited conversions, ranging from 60-90%. The residual monomer remains within the cured polymer network and can migrate and interact with its physiological environment. The methacrylic and especially the acrylic functional group are known to act as Michael acceptors and can therefore interact with physiological thiols and amines, e. g. of proteins or DNA molecules. [20], [21]

Thirdly, upon hydrolytic cleavage (meth)acrylic acid can be formed, possibly leading to a decrease of the pH value in the surrounding system. The response of a human body to such degradation products is either an inflammatory reaction or tissue necrosis in the worst case. [22], [23], [24]

<u>Motivation and outline</u>

In recent years, thiol-ene and thiol-yne systems have been explored as photoreactive and biocompatible resins. [25], [26], [27], [28] These step-growth polymers feature a delayed gelation point compared to (meth)acrylates. [29] Monomers and oligomers exhibit increased mobility for an extended amount of time while the curing reaction takes place, resulting in higher overall conversions. [26]The high conversions of this reaction type limit the migration of monomers to a minimum. Since internal stresses only start building up after the gelation point, the stresses induced by polymerization shrinkage can be released instead of being stored within the polymer network, thus making the polymer tougher than (meth)acrylates. [30], [31], [27] In addition, the network structure is highly uniform, which causes the glass transition regime to be well-defined. [29] In the case of thiol-yne systems, both the monomers as well as the degradation products show higher biocompatibility than (meth)acrylic systems. [25], [26] All in all, step-growth polymers combine high conversions and tough material behavior with good biocompatibility all in one material class.

Many traits of the step-growth polymerization are desirable for the photolithographic production of micro-sized elements. The delayed gel point as well as the absence of oxygen inhibition lead to an increased precision regarding the manufacturing of parts for medical devices, microfluidics or nanoimprint lithography. [32], [33], [34]

The greatest limitation for these innovative fields of application is the commercial availability of resin systems. Being a fairly new branch of research, thiol-yne derived resins have not been fully explored yet. [15] The catalog of monomers does not cover the growing demand for specialized applications in medicine and industry. In order to tackle this challenge, the strategy for the synthesis and material characterization of novel thiol-yne based compounds shall be presented within the scope of this thesis.

In the first approach, a bifunctional, commercially available acrylate was modified in a two-step reaction to completely replace the acrylate moieties with alkyne functional groups. In a second approach, Hydroxyethyl methacrylate was functionalized with an alkyne group to study its behavior as a part of a thiol-yne-methacrylate system. When cured with a thiol, the novel monomers are supposed to feature all the advantages of thiol-yne systems, including a delayed gelation point, high monomer conversions and low cytotoxicity while preserving the mechanical properties of their (meth)acrylate backbones.

2 Introduction

2.1 Materials for photopolymerization

2.1.1 Acrylates and methacrylates

Methacrylate and acrylate resins feature many desirable properties such as ambient curing, curing on demand, a high efficiency and speed as well as no requirement for solvents. Another advantage of (meth)acrylates are the large number of commercially available and well-established systems. However, these resins also exhibit a number of serious drawbacks, ranging from polymerization-induced shrinkage and high shrinkage stress [35], [36] to oxygen inhibition, skin irritation and a broad, undefined glass transition regime. [37], [30], [38], [39]

(Meth)acrylates undergo a radical chain-growth polymerization (Figure 2.1). In the case of photo-curable resins, a light sensitive photoinitiator is used to generate free radicals. These radicals can then attack a carbon-carbon double bond, effectively creating a carbon centered radical, which is capable of starting the next propagation step. Those systems reach the gelation point very fast and so the conversion of (meth)acrylate groups doesn't exceed 60 - 90 %. The early vitrification limits the mobility of monomers, which are therefore unable to find a reactive counterpart and remain within the network as residual monomer.
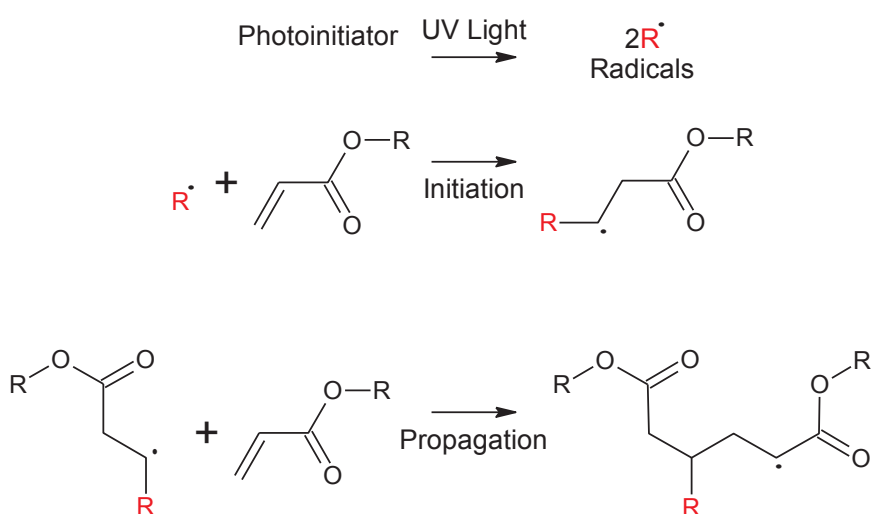

Figure 2.1: Radical mediated, photo induced chain-growth mechanism [69].

2.1.2 Thiol-ene click-reactions

1.) Photopolymerization

In 2001 a novel concept for highly selective and orthogonal reactions was reported by Sharpless et al.. [40], [41] The characteristics of these so-called click-reactions are high yields, nearly no side products, regio- and stereoselectivity, mild reaction conditions as well as insensitivity towards oxygen and moisture. [42] Hoyle and Bowman elaborately described the click-reaction of alkenes and thiols, which exhibits all the desirable features reported by Sharpless et al.. If the monomers are at least bifunctional, polymers and even three-dimensional networks can be created. This thiol-ene click-reaction follows a step-growth mechanism (Figure 2.2) [42]:

First, a free radical is generated through the illumination of a photoinitiator. In contrast to a chain-growth mechanism, this radical abstracts a hydrogen from a thiol instead of attacking a carbon-carbon double bond, creating a thiyl radical. The addition of such a thiyl radical to a carbon-carbon double bond leads to a carbon centered radical, which subsequently abstracts a hydrogen from another thiol functional group. On this way another thiyl radical is generated. It is worth to mention that no homopolymerization of the carbon-carbon double bonds occurs in an ideal step-growth polymerization. [43]
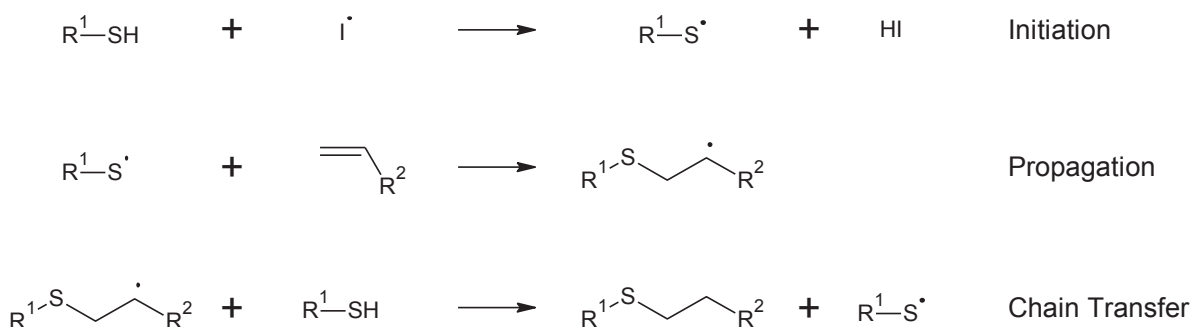

Figure 2.2: Radical mediated thiol-ene step-growth polymerization.

The step-growth polymerization mechanism has been proven to feature a delayed gelation point in comparison to the chain-growth mechanism. Moreover in Thiol-ene systems, the polymer network is more homogeneous and exhibits a much narrower glass transition regime than (meth)acrylate derived polymers. [29] The increased period of time, until reaching the gelation point, leads to a reduced shrinkage stress. [31], [30]

Thiol-ene reactions exhibit a comparatively low overall shrinkage of only 12-15 cm^3 mol^{-1} [44] per reacting double bond. This effect is caused by the uniform network architecture that stems from the step-growth polymerization mechanism. (Meth)acrylates show values up to 22-23 cm^3 mol^{-1} [45] per reacting double bond and therefore have a higher potential to build up internal stresses due to hindered shrinkage.

Besides a radical mediated thiol-ene reaction, thiols can also undergo a nucleophilic reaction with electron deficient alkenes such as acrylates, methacrylates, maleimides and others. This type of reaction is called Thiol-Michael reaction and can be started by a variety of catalysts like strong bases, metals, organometallic species and Lewis acids. [46] Since no radical mediated homopolymerization can occur in a Thiol-Michael reaction, the resulting polymer network can be different in comparison to a radical mediated thiol-ene reaction.

Two user-related drawbacks of thiol-ene systems are the distinct odor of thiols and the rather low storage stability of thiol-ene compounds. [31] In addition, the comparatively flexible thioether bonds as well as the rather low crosslink density lead to an overall soft material. In some cases, the glass transition temperature does not exceed room temperature, which poses severe limitations for this material class. [47], [48]

To overcome those limitations more rigid backbone structures can be implemented such as norbornenes or maleimides. Alternatively, the crosslink density can be increased by up to six times by using alkynes instead of alkenes in a so-called thiol-yne reaction. [49], [50], [51]

2.1.3   Thiol-yne polymerization reaction

The radical mediated step-growth polymerization of a thiol and an alkyne is depicted in Figure 2.3. At first, a thiyl radical reacts with a carbon-carbon triple bond, generating a carbon centered radical. Subsequently this newly formed radical abstracts a hydrogen from a thiol functional group. This leads to the formation of a vinyl sulfide moiety which is capable of reacting with another thiol monomer according to the thiol-ene reaction mechanism that is mentioned above. As a result, thiol-yne networks exhibit an increased cross-link density, a higher glass transition temperature and improved mechanical properties compared to thiol-ene networks. [52], [53], [54]
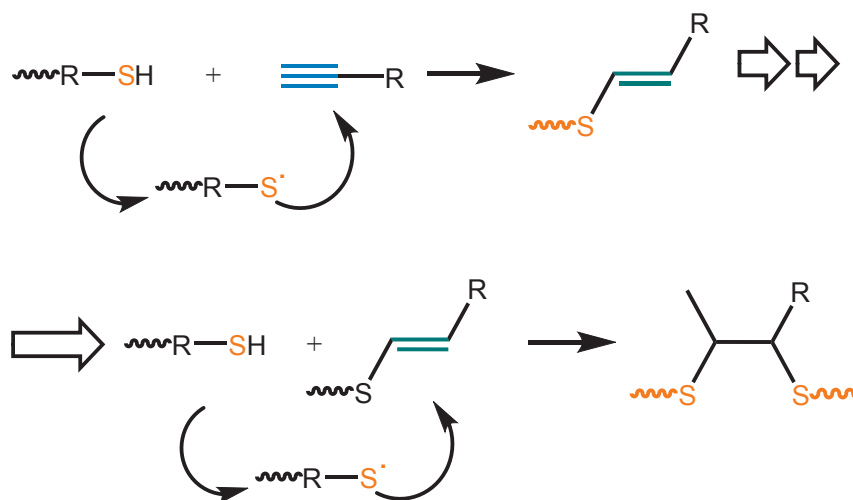
Introduction

Figure 2.3: Radical mediated thiol-yne step-growth polymerization.

2.1.4 Network properties of thiol-yne-methacrylate systems

Through the addition of (meth)acrylates to thiol-ene or thiol-yne systems a ternary system with unique reaction kinetics (depicted in Figure 2.4) and network formation processes is created. In such cases, a competition arises between the (meth)acrylate homopolymerization and the chain transfer to a thiol, thus promoting the thiol-ene or thiol-yne step growth polymerization. [55]
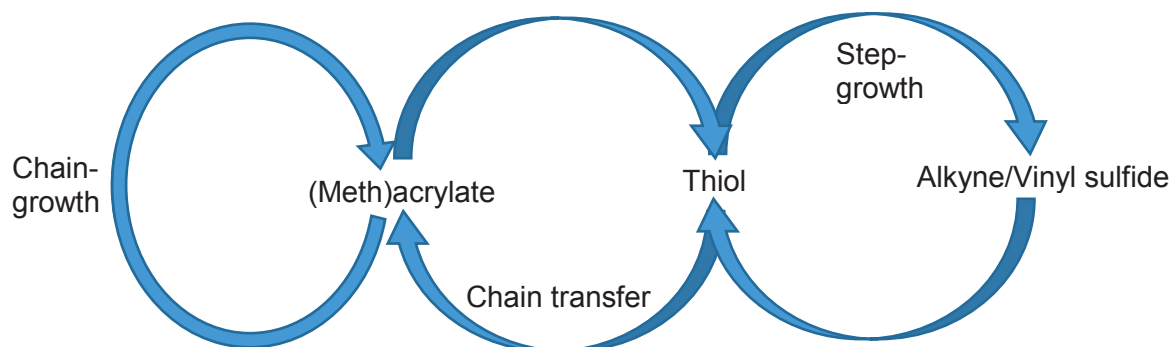

Figure 2.4: Competition between chain-growth, chain transfer and step-growth mechanism in a thiol-yne-(meth)acrylate ternary system.

By varying the amount and structure of the monomers, a favorable and tailor-made combination of network properties can be achieved. Lee et al. [56] have reported a significant decrease in shrinkage stress of methacrylate systems by incorporating a thiol-allyl ether component. In that case, a two-stage hybrid polymerization can be observed. While the

methacrylate domains already reach higher conversions, the thiol-ene regimes are still composed of relatively small oligomers with enough mobility to act as plasticizing solvent during the early stages. Up to this point no internal stresses are created. Afterwards, internal stresses start to build up at a comparable rate to thiol-ene systems. Through this combination of materials, the methacrylate shrinkage stresses could be reduced by 50% while maintaining a high glass transition temperature of 100 °C. The different stages of the network evolution are depicted in Figure 2.5.
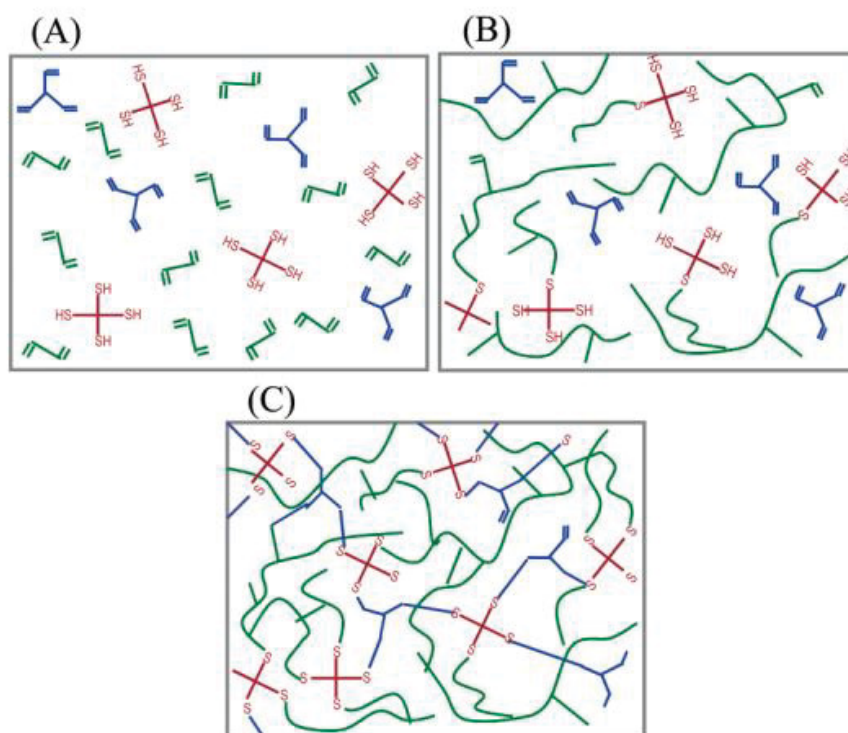

Figure 2.5: Network evolution of a thiol-allyl ether-methacrylat system: (A) Before polymerization, (B) formation of methacrylate domains, (C) formation of thiol-ene domains. [56]

Another study by Bowman et al. has shown significant increases in T_g and modulus (up to 44%) of thiol-yne systems by adding a methacrylate component. However, low levels of shrinkage stress could be maintained due to the fact that the thiol-yne component comprises a delayed gelation. Because a large portion of the total amount of shrinkage takes place before the gel point is reached, most stresses can be released instead of being stored within the solid network. [57], [58]

Comparable ternary systems have significant potential for materials with tailor made network properties regarding the glass transition temperature, mechanical properties and shrinkage stresses. [58]

2.2 Photo Differential Scanning Calorimetry (Photo-DSC) as an efficient tool to investigate polymerization reaction rates

DSC is a simple and fast method to determine the absorbed or released heat of a sample during heating, cooling or illumination. The difference in temperature between a reference and sample crucible is used to calculate the absorbed or released amount of heat as a function of time and temperature. The basic DSC test setup is depicted in Figure 2.6.
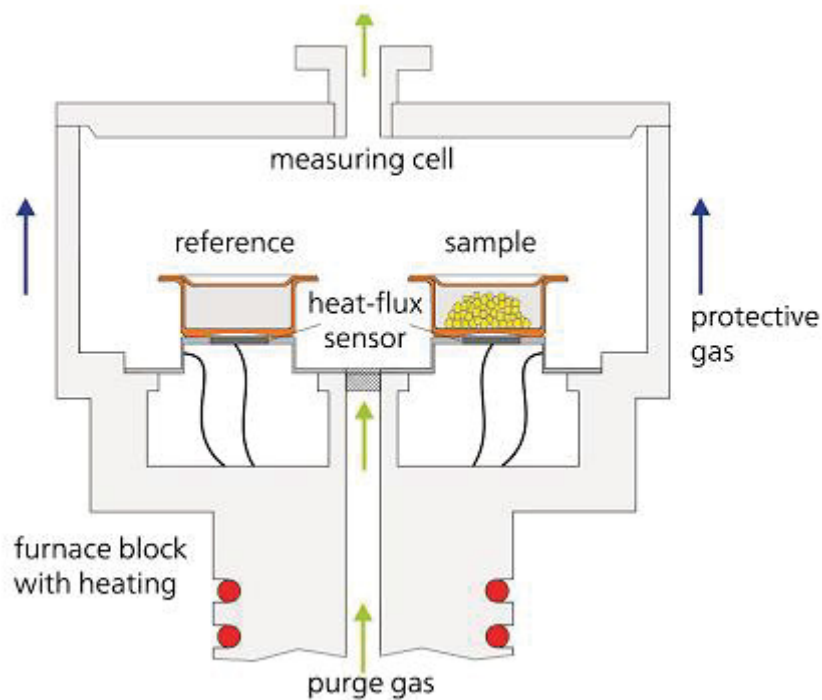

Figure 2.6: Schematic of a basic DSC test setup. [59]

In the case of a Photo-DSC setup, the temperature of both crucibles is kept while the sample is illuminated with UV-light. If a light induced curing reaction takes place, the released heat of polymerization can be monitored. As depicted in Figure 2.7, the reaction enthalpy ΔH can be obtained through integration of the curve. If the theoretical standard enthalpy of reaction ΔH_{th} is known, monomer conversion (DC) can be estimated according to equation (1).

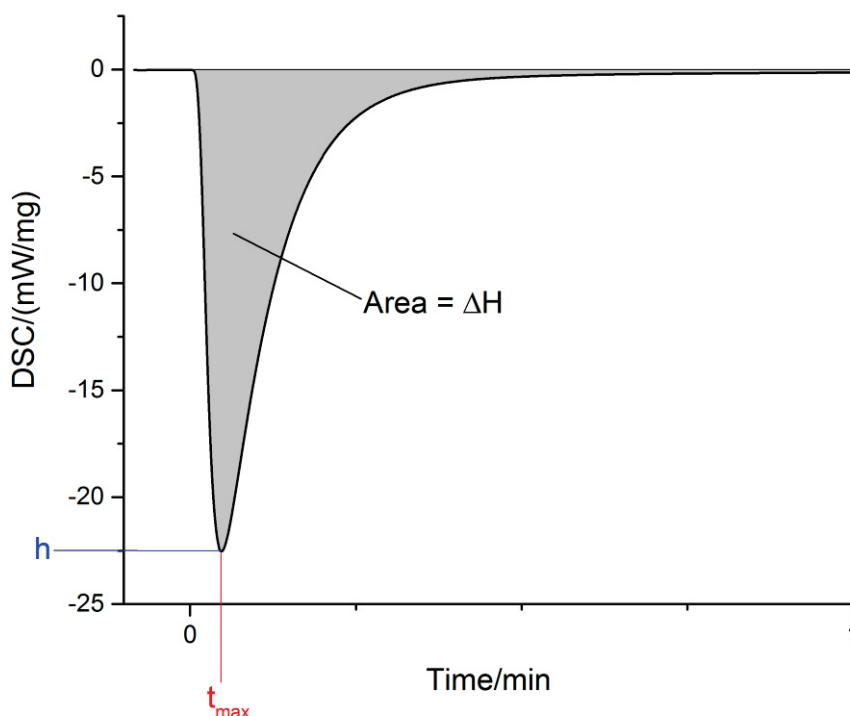$$DC = \frac{\Delta H}{\Delta H_{th}} \tag{1}$$

Figure 2.7: Analysis of a Photo-DSC curve.

The time to reach the maximum of the reaction heat (t_{max}) and the maximum peak height h can be used as a measure for the reaction rate of monomer systems. In this work, t_{max} was used to evaluate the reaction rates of various compounds. Since ΔH_{th} of the novel monomers is unknown, the monomer conversions have to be investigated by real-time Fourier Transform Infrared Spectroscopy (FTIR) instead.

2.3 Investigation of the Crack Tip Opening Angle (CTOA) to evaluate material toughness

The crack tip opening angle (CTOA) is defined as the average angle of the two crack surfaces measured at a point 1 mm behind the crack tip and characterizes stable crack growth of thin walled materials in low constraint conditions. After an initiation phase, the CTOA stays relatively constant throughout a wide range of crack extension while the crack growth remains stable. Originally designed for thin walled sheet metals, the criterion can also be used to qualitatively compare polymers in regards of their toughness. While tough and more ductile materials can endure larger opening angles, the CTOA of brittle materials can only reach small values before the failure of the test specimen. [60]

2.4 **Stereolithography**

Stereolithography is an innovative 3-D printing technique for photopolymers that is used for manufacturing complex three-dimensional objects. The process is already known since the 1980s as a rapid prototyping method for the automotive industry. [61], [62] Despite the introduction of other processing methods in more recent years (e. g. selective laser sintering, fused deposition modeling etc.) stereolithography still comprises the best resolutions while providing incredible freedom of design. The lowest possible resolutions range down to 10 µm and due to the unique shaping process almost every geometry is printable. The machine itself consists of a movable platform reaching into a basin of monomer resin and a UV-light source to illuminate the transparent bottom of the resin reservoir. The selective curing of one monomer layer is either performed as a series of punctual illuminations by a UV-laser beam (direct laser writing) or by a digital light projector (DLP) to illuminate a complete layer of resin at once. Control over the power of the light source and the duration of illumination is crucial, as those parameters heavily influence the layer thickness and therefore the quality of the parts. After the first layer has solidified upon the platform, the construct is moved in vertical direction so a fresh layer of resin is applied. Through the subsequent repetition of illumination and vertical movement, the three-dimensional part is formed layer by layer. The raw part is then washed and post cured by UV light and/or elevated temperature to remove excess resin and to increase monomer conversion and crosslink density. [63]
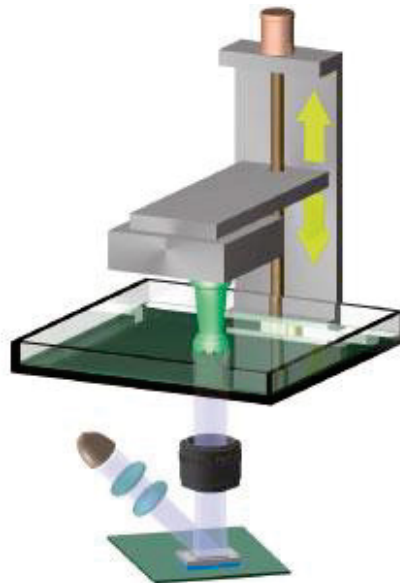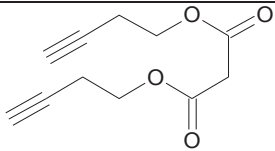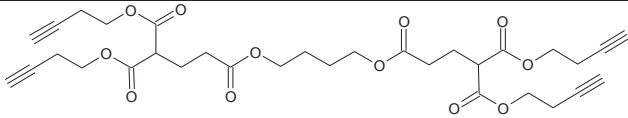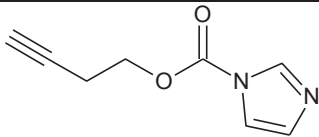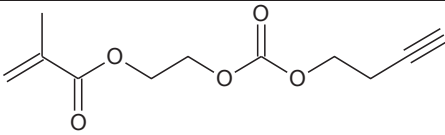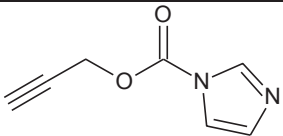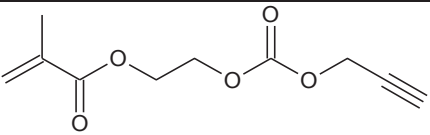

Figure 2.8: Basic machinery for stereolithography.

3 Results and discussion

3.1 Monomers synthesis

The monomer structures, the full names and respective abbreviations of the synthesized monomers and their intermediates are depicted in Table 3.1. Intermediates are labeled with lowercase letters.

Table 3.1: Overview of synthesized monomers and their intermediates.

Abbreviation	Chemical structure	Full name
Ia		Malonyldibutynylester
I		Butanedioldipropionate-di-malonyldibutynylester
IIa		But-3-yn-1-yl-1H-imidazole-1-carboxylate
II		2-(((But-3-yn-1yloxy)ethyl methacrylate
IIIa		Prop-2-yn-1-yl-1H-imidazole-1-carboxylate
III		2-(((Prop-2-yn-1-yloxy)carbonyl)oxy)ethyl methacrylate

Results and discussion

3.1.1 Synthesis of Butanedioldipropionate-di-malonyldibutynylester (I)

Malonyldibutynylester was obtained through an esterification reaction of Malonyl chloride with 3-Butyn-1-ol using catalytic amounts of Pyridine. The crude product was purified by distillation, which led to a good yield of 81.5 %.
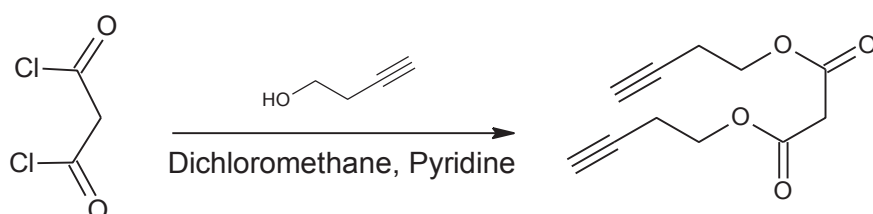

Figure 3.1: Synthesis of Malonyldibutynylester through an esterification reaction.

Malonyldibutynylester was attached to a backbone of 1,4-Butanediol diacrylate via a Michael addition in the presence of catalytic amounts of Tributylphosphine. In the process, the bifunctional acrylate was successfully converted into a tetrafunctional alkyne. The crude product could not be purified by distillation because the compound started decomposing before evaporating. Instead, column chromatography had to be used to obtain the product in a yield of 67.0 %.
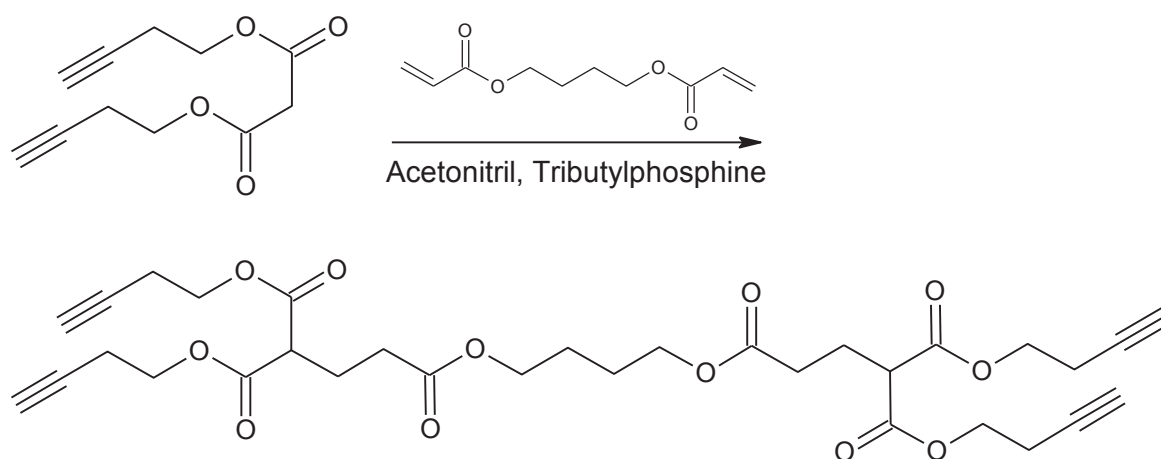

Figure 3.2: Synthesis of Butanedioldipropionate-di-malonyldibutynylester via a Michael addition reaction.

An alternative synthesis was investigated in order to provide a bifunctional monomer. In a first step, Cyanoacetic acid was esterified with 3-Butyn-1-ol, using a combination of 4-(Dimethylamino)pyridine (DMAP) and N,N′-Dicyclohexylcarbodiimide (DCC) as catalytic

system. However, ^{1}H-NMR spectra suggest that the second reaction step was not successful, since no consumption of acrylate double bonds could be observed.
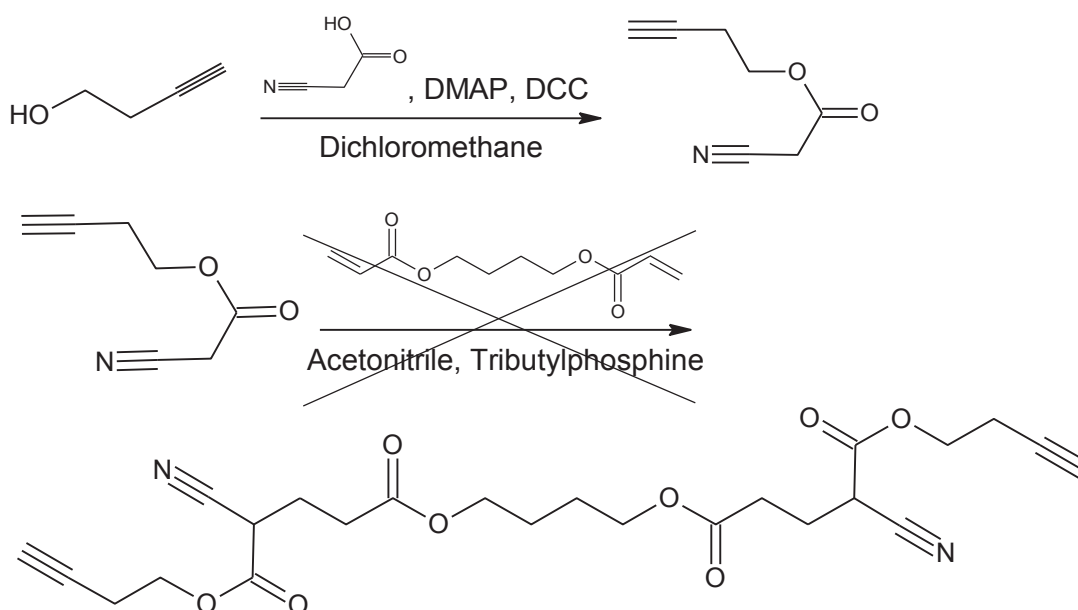

Figure 3.3: Failed synthesis of a bifunctional alkyne of in a two-step reaction.

3.1.2 Synthesis of 2-(((But-3-yn-1-yloxy)ethyl methacrylate (II) and 2-(((Prop-2-yn-1-yloxy)carbonyl)oxy)ethyl methacrylate (III)

Using catalytic amounts of KOH 3-Butyn-1-ol and an excess amount of 1,1′-Carbonyldiimidazole (CDI) were reacted to But-3-yn-1-yl-1H-imidazole-1-carboxylate. When being exposed to water, CDI immediately decomposes into CO_2 and Imidazole. Due to the good water solubility of Imidazole, it can be easily extracted. The crude product was washed with water and dried over Na_2SO_4 as only means of purification. Thanks to this efficient method of purification an excellent yield of 93.3 % could be achieved.
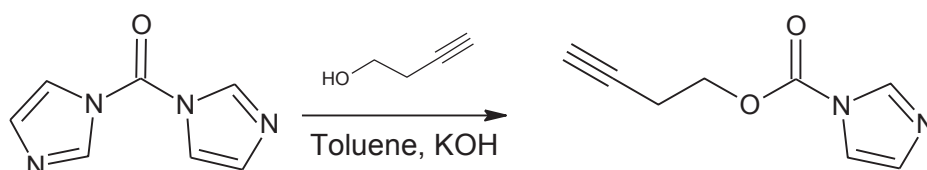

Figure 3.4: Synthesis of But-3-yn-1-yl-1H-imidazole-1-carboxylate.

Results and discussion

In the second reaction step, But-3-yn-1-yl-1H-imidazole-1-carboxylate and Hydroxyethyl methacrylate (HEMA) were reacted to 2-(((But-3-yn-1-yloxy)ethyl methacrylate. The crude product had to be purified by column chromatography, resulting in a yield of 71.2 %.
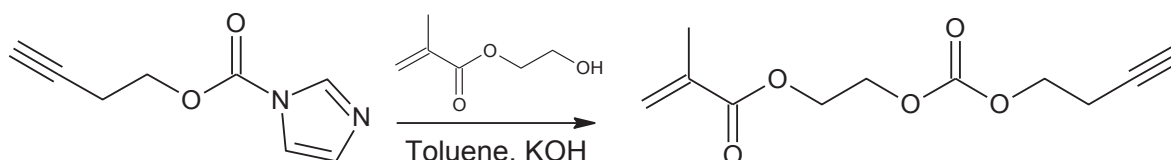

Figure 3.5: Synthesis of 2-(((But-3-yn-1-yloxy)ethyl methacrylate.

Through an analogous procedure 2-((((Prop-2-yn-1-yloxy)carbonyl)oxy)ethyl methacrylate was successfully synthesized by using Propargyl alcohol instead of 3-Butyn-1-ol. The yields in both steps (90.5 % and 60.7 %) turned out to be slightly lower than in the previous synthesis of 2-(((But-3-yn-1-yloxy)ethyl methacrylate. This can be explained by the higher reactivity of the propargyl moiety which causes the formation of more side products.
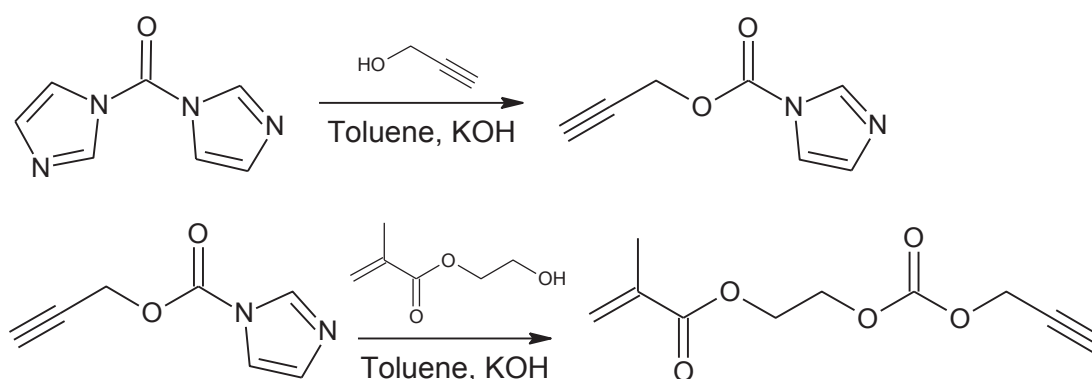

Figure 3.6: Synthesis of 2-((((Prop-2-yn-1-yloxy)carbonyl)oxy)ethyl methacrylate in a two-step reaction.

3.2 **Preparation of model formulations**

For the investigation of photoreactivity and monomer conversions various formulations of the novel monomers were used. The components of these mixtures as well as their abbreviations are listed in Table 3.2. To all resin formulations 3 wt% Irgacure TPO-L was added as photoinitiator. The photopolymers of selected resin formulations were used for dynamic mechanical analysis and the measurement of the crack tip opening angle.

Table 3.2: Components of photoreactive formulations.

Abbreviation	Components*
Ref_PETMP_Alkyne	1,4- Butanediol dipropargylcarbonate (33.3 %) Pentaerythritol tetrakis(3-mercaptopropionate) (33.3 %) 1,4-Butanediol dimethacrylate (33.3 %)
Ref_PETMP_Both	1,4- Butanediol dipropargylcarbonate (28.6 %) Pentaerythritol tetrakis(3-mercaptopropionate) (42.8 %) 1,4-Butanediol dimethacrylate (28.6 %)
Ⅰ_PETMP	Butanedioldipropionate-di-malonyldibutynylester (33.3 %) Pentaerythritol tetrakis(3-mercaptopropionate) (66.7 %)
Ⅱ_PETMP_Alkyne	2-(((But-3-yn-1yloxy)ethyl methacrylate (66.7 %) Pentaerythritol tetrakis(3-mercaptopropionate) (33.3 %)
Ⅱ_PETMP_Both	2-(((But-3-yn-1yloxy)ethyl methacrylate (57.1 %) Pentaerythritol tetrakis(3-mercaptopropionate) (42.9 %)
Ⅱ_PETMP_UDMA_30	2-(((But-3-yn-1yloxy)ethyl methacrylate (42.0 %) Pentaerythritol tetrakis(3-mercaptopropionate) (45.4 %) Urethane dimethacrylate (12.6 %)
Ⅱ_PETMP_UDMA_30_Ex	2-(((But-3-yn-1yloxy)ethyl methacrylate (45.5 %) Pentaerythritol tetrakis(3-mercaptopropionate) (40.9 %) Urethane dimethacrylate (13.6 %)

Results and discussion

II _PETMP_UDMA_40	2-(((But-3-yn-1yloxy)ethyl methacrylate (39.4 %) Pentaerythritol tetrakis(3-mercaptopropionate) (44.9 %) Urethane dimethacrylate (15.7 %)
II _PETMP_UDMA_40_Ex	2-(((But-3-yn-1yloxy)ethyl methacrylate (43.5 %) Pentaerythritol tetrakis(3-mercaptopropionate) (39.1 %) Urethane dimethacrylate (17.4 %)
II _PETMP_UDMA_50	2-(((But-3-yn-1yloxy)ethyl methacrylate (33.3 %) Pentaerythritol tetrakis(3-mercaptopropionate) (50.0 %) Urethane dimethacrylate (16.7 %)
II _PETMP_UDMA_50_Ex	2-(((But-3-yn-1yloxy)ethyl methacrylate (41.7 %) Pentaerythritol tetrakis(3-mercaptopropionate) (37.5 %) Urethane dimethacrylate (20.8 %)
III_PETMP_Alkyne	2-(((Prop-2-yn-1-yloxy)carbonyl)oxy)ethyl methacrylate (66.6 %) Pentaerythritol tetrakis(3-mercaptopropionate) (33.3 %)
III_PETMP_Both	2-(((Prop-2-yn-1-yloxy)carbonyl)oxy)ethyl methacrylate (57.1 %) Pentaerythritol tetrakis(3-mercaptopropionate) (42.9 %)
BdoAc_Pure	Butandediol diacrylate (100 %)
UDMA_Pure	Urethane dimethacrylate (100 %)

*specifications in mole percent

3.3 Investigation of the photoreactivity through Photo-Differential scanning calorimetry (Photo-DSC) measurements

Whether for printing, coating or photolithographic applications, the curing rate is always one of the most defining properties of photoactive resins. The synthesized tetrafunctional alkyne and the two alkyne-methacrylate hybrid monomers were investigated with photo-DSC in order to evaluate their curing rate in comparison to methacrylates and other ternary systems. The time necessary to reach the maximum of the polymerization enthalpy (t_{max}) was utilized to compare the competitiveness of the novel monomers.

In these studies, Pentaerythritol tetrakis(3-mercaptopropionate) (PETMP) was used in combination with Butanedioldipropionate-di-malonyldibutynylester (I_PETMP), 2-(((But-3-yn-1yloxy)ethyl methacrylate (II_PETMP) and 2-(((Prop-2-yn-1-yloxy)carbonyl)oxy)ethyl methacrylate (III_PETMP).

In order to provide additional information on the curing behavior of the synthesized hybrid monomers, stochiometric and non-stochiometric compounds of the ternary systems were studied. On the one hand, a stoichiometric amount of thiol was provided to fully saturate both the alkyne as well as the methacrylate groups (labeled with _Both). On the other hand, only enough thiol was provided to react with the alkyne groups (labeled _Alkyne), while the entirety of the methacrylate groups (theoretically) has to rely on homopolymerization. In real systems a thiol-ene reaction between methacrylate and thiol groups can occur, which potentially limits the supply of thiol for a thiol-yne reaction.

Diurethane dimethacrylate (UDMA_Pure) was used as a reference substance for systems based on (meth)acrylates. These systems are well known for their fast reaction rate. It is therefore one of the major challenges for novel compounds to reach similar levels of speed.

The hybrid monomers combine a methacrylate and an alkyne moiety in one molecule. In comparison to conventional ternary formulations, featuring separate components for alkyne and methacrylate, differences in photoreactivity and monomer conversion are possible. In order to study the unique features of the hybrid monomers, a reference system consisting of 1,4-Butanediol dipropargylcarbonate, PETMP and 1,4-Butanediol dimethacrylate (Ref_PETMP) was also investigated so the results could be compared.

The plots of the photo-DSC measurements are depicted in Figure 3.7 to Figure 3.11, while a summary of the results is presented in Table 3.3.

Results and discussion

Table 3.3: Results of Photo-DSC measurements for compounds containing PETMP and Butanedioldipropionate-di-malonyldibutynylester, 2-(((But-3-yn-1yloxy)ethyl methacrylate and 2-(((Prop-2-yn-1yloxy)ethyl methacrylate compared to UDMA.

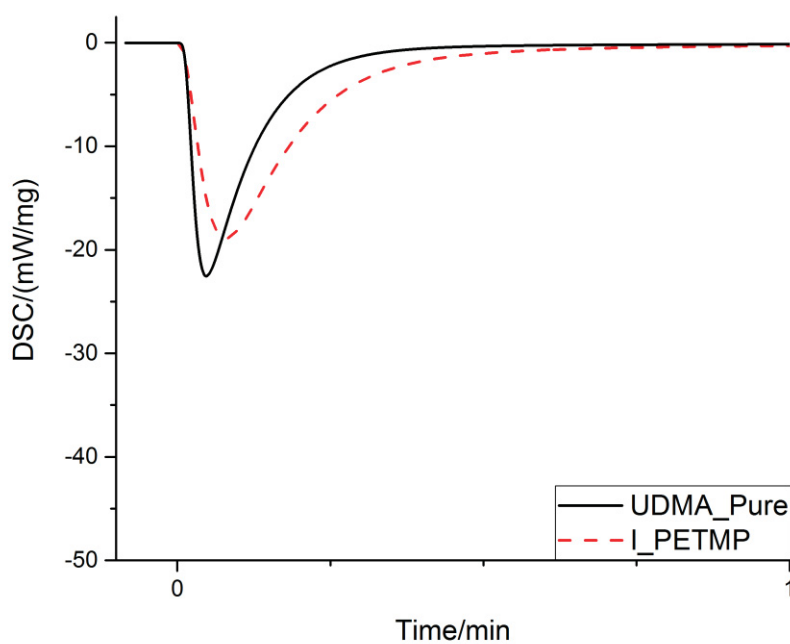| Compound	t_{max} [s]
UDMA_pure	2.82
Ref_PETMP_Alkyne	13.74
Ref_PETMP_Both	10.62
I_PETMP	4.74
II_PETMP_Alkyne	16.44
II_PETMP_Both	11.82
III_PETMP_Alkyne	17.64
III_PETMP_Both	13.44

Figure 3.7: Photo-DSC plots of a stoichiometric thiol-yne system consisting of Butanedioldipropionate-di-malonyldibutynylester and PETMP in comparison to pure UDMA.

The thiol-yne system shows good results, achieving a t_{max} of 4.74 s, therefore almost reaching the reaction rate of pure UDMA at 2.82 s.
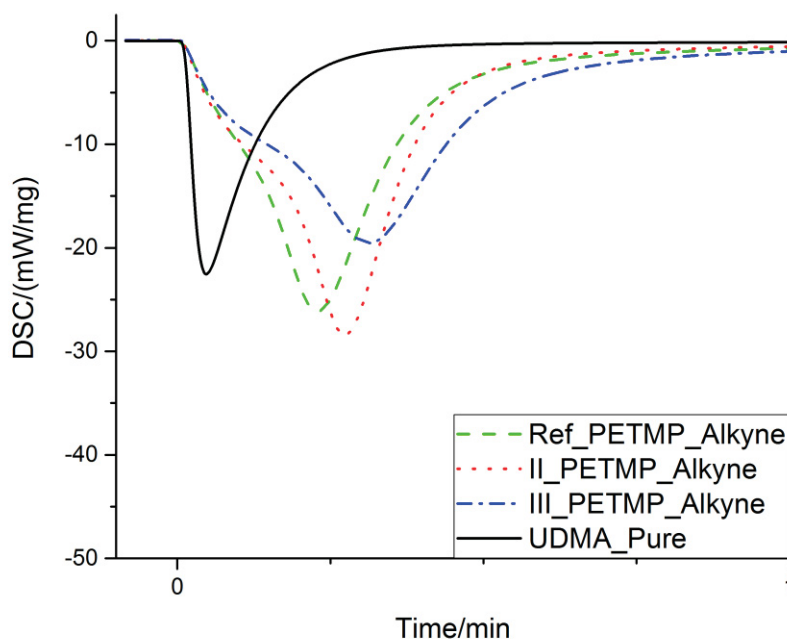
Results and discussion

Figure 3.8: Photo-DSC plots of non-stoichiometric ternary systems consisting of 1,4- Butanediol dipropargylcarbonate and 1,4-Butanediol dimethacrylate (ref.), 2-(((But-3-yn-1yloxy)ethyl methacrylate, 2-(((Prop-2-yn-1yloxy)ethyl methacrylate and PETMP in comparison to pure UDMA.

In comparison to UDMA, all ternary systems exhibit a rather slow reaction rate, up to 5 times slower for the non-stoichiometric compounds. This seems to be a downside of ternary systems compounds in general and not a specific drawback attributed to the hybrid nature of the novel monomers because the reference system is also significantly slower than UDMA. One possible explanation is an increase in viscosity as the oligomers simultaneously grow larger and limit the mobility of each other. The particularly fast chain-growth mechanism of UDMA is less affected by this phenomenon. Since propagation only occurs on chain ends, the surrounding domains are rich in low molecular monomer with enough mobility to encounter a reactive site.
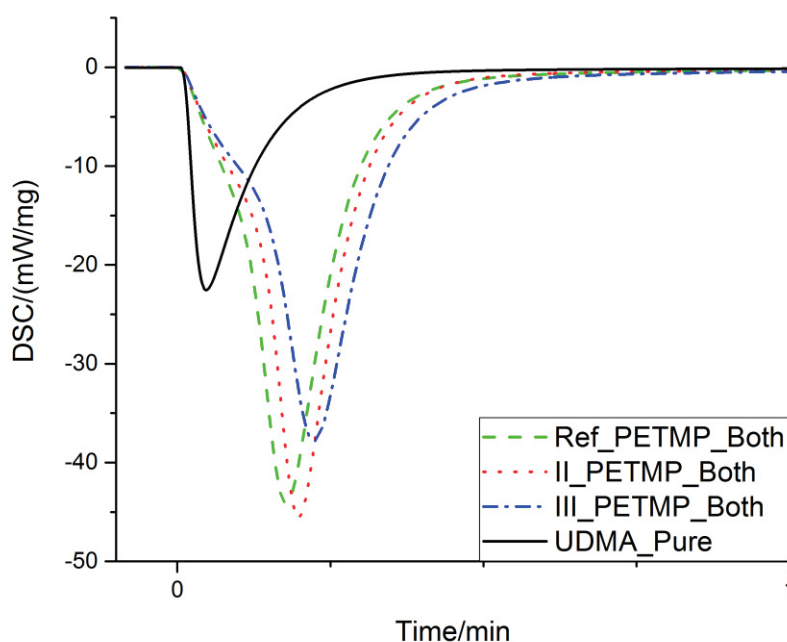
Results and discussion

Figure 3.9: Photo-DSC plots of stoichiometric ternary systems consisting of 1,4- Butanediol dipropargylcarbonate and 1,4-Butanediol dimethacrylate (ref.), 2-(((But-3-yn-1yloxy)ethyl methacrylate, 2-(((Prop-2-yn-1yloxy)ethyl methacrylate and PETMP in comparison to pure UDMA.

The non-stochiometric systems are notably slower than their stoichiometric counterparts by up to 4.62 s in the case of II_PETMP. The conversion of methacrylate can take place with or without a thiyl radical, following either a thiol-ene reaction or a methacrylate homopolymerization. However, the conversion of alkyne groups depends on a thiyl radical to start a thiol-yne reaction. In the non-stoichiometric systems the supply of thiol (and therefore thiyl radicals during illumination) is more limited. As a result, encountering the reactive thiyl species is statistically less likely and so the overall reaction time until monomer depletion is increased.

On the other hand, the stoichiometric systems are faster in every case. The reason for this is the generous supply of thiol that can readily react with alkynes as well as methacrylates, so that the curing reaction can take place until all monomers are depleted.

In both, the stoichiometric and the non-stoichiometric experiment, II_PETMP is slightly faster than III_PETMP. The butynyl carbonate features an additional CH_2 group which decreases the inductive effect of the carbonate group on the terminal alkyne, therefore increasing its photoreactivity. [25] However, both hybrid molecules exhibit slower reaction rates than the reference system.

Results and discussion

3.3.1 Improvement of reaction rate in a ternary system of 2-(((But-3-yn-1-yloxy)ethyl methacrylate

Since for many applications a fast curing rate is favorable, further experiments had to be carried out to raise the reaction rates of the hybrid molecules to higher levels. In in order to increase the reaction rate UDMA was added at certain amounts:

To a system of 2-(((But-3-yn-1yloxy)ethyl methacrylate 30, 40 and 50 molar percent UDMA were added. 1.2 equivalents of PETMP regarding all functional groups were then added to form a stoichiometric system with a slight excess of PETMP (labeled Ⅱ_PETMP_UDMA_30/40/50).

In order to create a non-stoichiometric compound, 1.2 equivalents of PETMP was added to the hybrid monomer 2-(((But-3-yn-1yloxy)ethyl methacrylate. An excess amount of UDMA (labeled with _Ex) was then added, again comprising of 30, 40 and 50 molar percent referring to the amount of the hybrid monomer. This effectively creates a system with a lack of thiol, thus inducing a competition between thiol-yne and thiol-ene reaction, while methacrylate homopolymerization takes place simultaneously.

Table 3.4: Results of Photo-DSC for compounds containing 2-(((But-3-yn-1yloxy)ethyl methacrylate and 2-(((Prop-2-yn-1yloxy)ethyl methacrylate with PETMP and UDMA compared to pure UDMA.

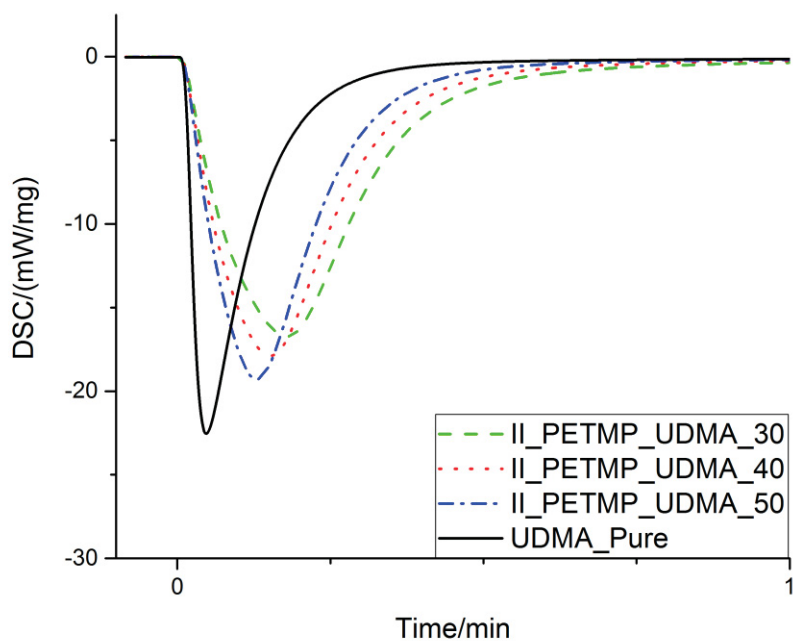| Compound	t_{max} [s]
UDMA_Pure	2.82
Ⅱ_PETMP_UDMA_30	10.74
Ⅱ_PETMP_UDMA_30_Ex	10.62
Ⅱ_PETMP_UDMA_40	9.12
Ⅱ_PETMP_UDMA_40_Ex	8.94
Ⅱ_PETMP_UDMA_50	7.86
Ⅱ_PETMP_UDMA_50_Ex	7.62

Results and discussion

Figure 3.10: Photo-DSC plots of stoichiometric ternary systems consisting of 2-(((But-3-yn-1yloxy)ethyl methacrylate, PETMP and UDMA in comparison to pure UDMA.
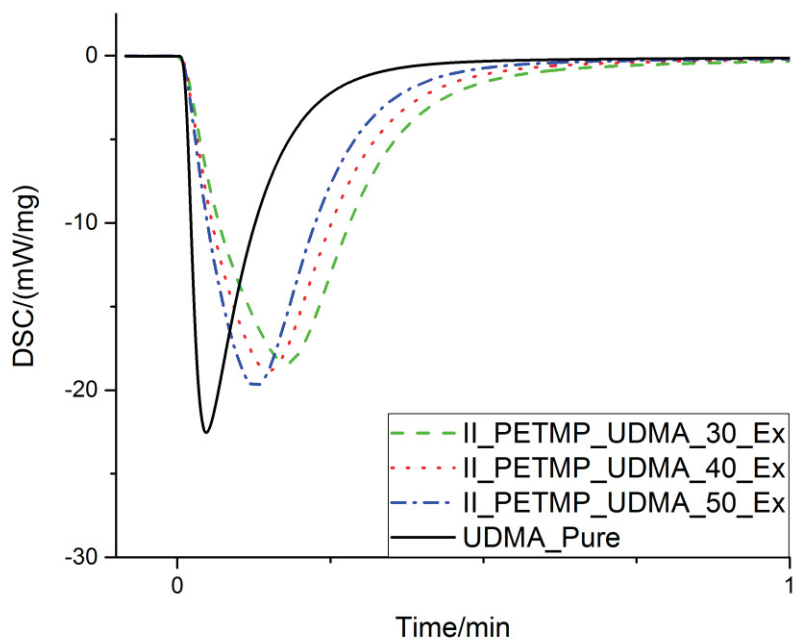

Figure 3.11: Photo-DSC plots of ternary systems consisting of 2-(((But-3-yn-1yloxy)ethyl methacrylate, PETMP and an excess of UDMA in comparison to pure UDMA.

Results and discussion

Although the systems containing excess amounts of UDMA tend to be slightly faster than the stoichiometric systems, the main influence factor on the reaction rate is the overall amount of UDMA. Although the velocity levels of pure UDMA cannot be matched yet, a significant influence towards faster reaction rates can be observed. The addition of up to 50 % UDMA leads to a reduction of t_{max} by up to 35.5 %, proving that the addition of UDMA to existing ternary compounds is an effective way to increase reaction rate.

3.4 Investigation of monomer conversion through real-time FTIR-spectroscopy

The amount of leachable monomer is directly affected by the monomer conversion. Especially for biomedical devices the levels of residual monomer should be reduced to a minimum in order to ensure good biocompatibility. One of the major problems of (Meth)acrylate systems is their comparably low conversions (60-90 %), which are mainly attributed to an early gelation point. By adding other substances such as thiols, the gelation point can be delayed. [31] In this context, thiol and alkyne components have also been added to alter the network formation process in a beneficial way.

The conversions of systems containing Butanedioldipropionate-di-malonyldibutynylester and PETMP (I_PETMP), 2-(((But-3-yn-1-yloxy)ethyl methacrylate and PETMP (II_PETMP) and 2-(((Prop-2-yn-1yloxy)ethyl methacrylate and PETMP (III_PETMP) were investigated by real-time FTIR-spectroscopy.

As discussed in the previous section, the addition of UDMA is capable of improving the reaction rate. Now real-time FTIR spectroscopy shall determine if adding UDMA to formulations influences conversion in a negative way by advancing the gelation point.

The peaks of the alkyne C≡H stretch ($\sim$ 3280 cm^{-1}), the thiol S-H stretch ($\sim$ 2560 cm^{-1}) and the acrylate C=C stretch ($\sim$ 1640 cm^{-1}) were used to monitor the conversion of functional groups over time. The integral area of the peaks during illumination was referenced with the initial value to show the consumption of monomer and follow the progress of the curing process.

Monomer conversion in various systems are depicted in Figure 3.12 to Figure 3.18, whereas a summary of the results is shown in Table 3.5 and Table 3.6.

Results and discussion

Table 3.5: Conversions of alkyne, thiol and methacrylate in ternary systems after 3 minutes of illumination and after thermal post-curing.

Compound	Conversion after 3 min [%]			Conversion after post-curing [%]		
	Alkyne	Thiol	Methacrylate	Alkyne	Thiol	Methacrylate
UDMA_Pure			54.7			97.8
Ref_PETMP_Alkyne	47.1	61.3	83.5	49.8	64.7	83.7
Ref_PETMP_Both	83.5	70.4	89.4	86.1	71.3	89.4
I_PETMP*	97.4	63.2				
II_PETMP_Alkyne	56.5	70.7	85.8	58.4	71.7	86.2
II_PETMP_Both	93.1	71.3	91.9	93.1	74.2	92.9
III_PETMP_Alkyne	64.8	78.3	92.1	69.5	78.3	93.4
III_PETMP_Both	94.0	69.6	100	95.3	71.4	100.0

* illuminated for only 80 seconds, no post-curing
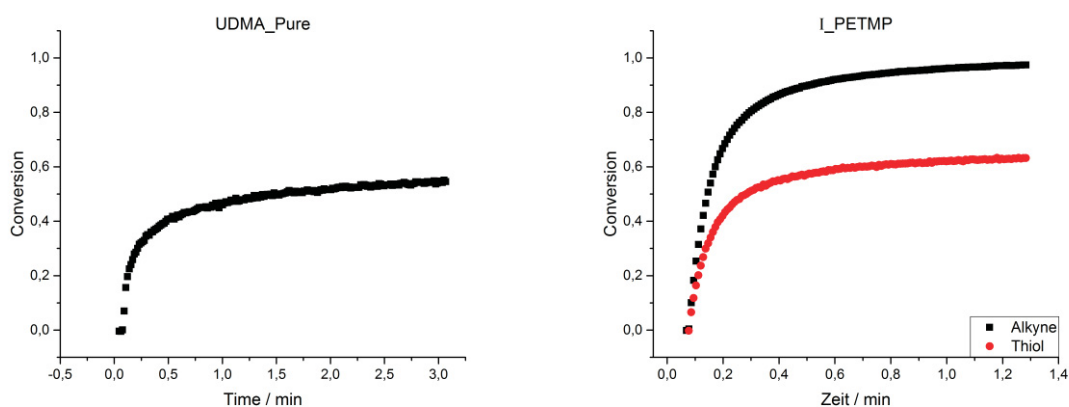
Figure 3.12: Conversion of methacrylate groups in pure UDMA (left) and conversions of alkyne and thiol groups in a binary system consisting of Butanedioldipropionate-di-malonyldibutynylester and PETMP (right).
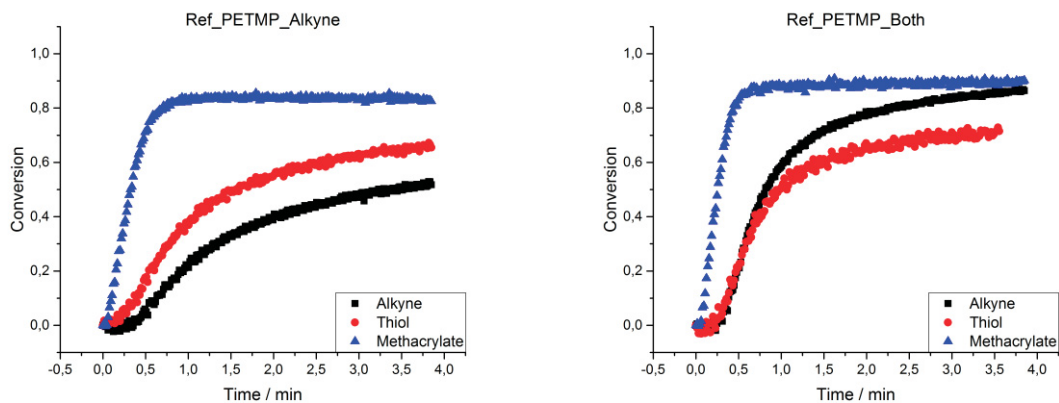
Results and discussion

Figure 3.13: Conversions of alkyne, thiol and methacrylate groups in a non-stoichiometric (left) and a stoichiometric (right) ternary system consisting of 1,4- Butanediol dipropargylcarbonate, PETMP and 1,4-Butanediol dimethacrylate.
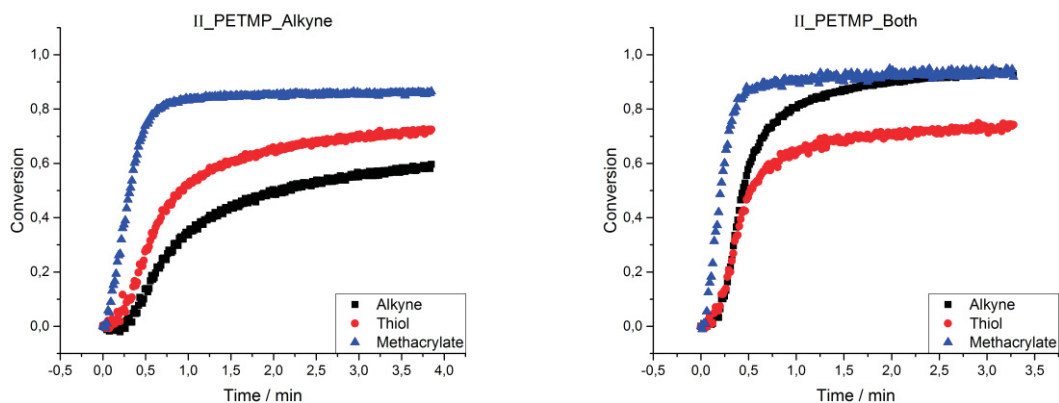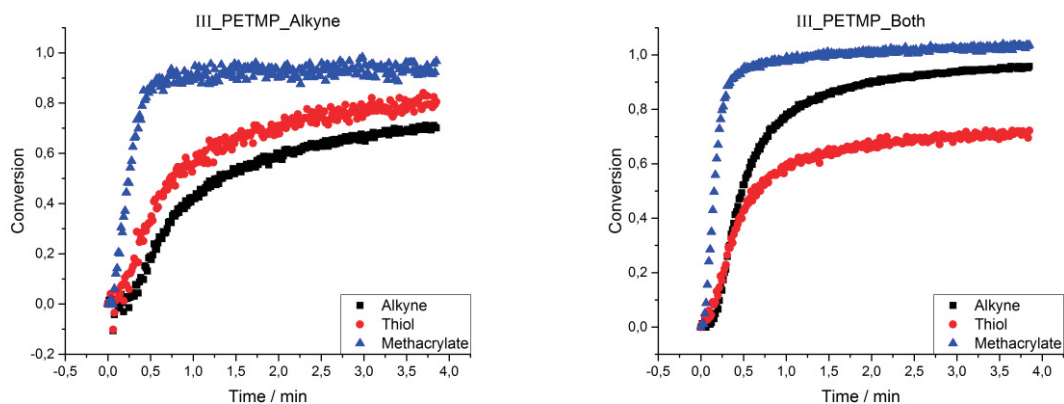

Figure 3.14: Conversions of alkyne, thiol and methacrylate groups in a non-stoichiometric (left) and a stoichiometric (right) ternary system consisting of 2-(((But-3-yn-1yloxy)ethyl methacrylate and PETMP.

Figure 3.15: Conversions of alkyne, thiol and methacrylate groups in a non-stoichiometric (left) and a stoichiometric (right) ternary system consisting of 2-(((Prop-2-yn-1yloxy)ethyl methacrylate and PETMP.

Results and discussion

The binary thiol-yne system exhibits almost complete alkyne conversion (97.4 %) after only 80 seconds of illumination, so that no post-curing step is required. The thiol component on the other hand only reaches 63.2 % conversion, suggesting that no complete thiol-yne reaction takes place. One possible explanation for this phenomenon could be a radical mediated homopolymerization of the Vinyl sulfide intermediate.

Pure UDMA shows very poor conversion of only 54.7 % after the illumination process. A thermal post-curing step is required to increase the conversion to 97.8 %. When being added to a thiol-yne compound, the conversion of UDMA drastically increases, especially during the first 60 seconds of curing.

The conversion of methacrylate in ternary systems is surprisingly high, suggesting that the gelation point has been notably delayed in comparison to ordinary methacrylates. As a result, monomers and oligomers exhibit higher mobility for a longer period of time before vitrification finally takes place. Excellent conversions even up to 100 % are possible.

Regarding the thiol-yne-methacrylate ternary compounds, a strong influence of the systems' stoichiometries is observed. In the non-stoichiometric systems (_Alkyne) parts of the thiol groups are consumed by thiol-ene reaction with methacrylate groups and is no longer available as reaction partner for the alkyne. Since alkynes cannot undergo homopolymerization in the prevailing circumstances, the conversion is limited and does not exceed 70 % in any of the given cases, even after thermal post-curing.

In contrast, alkyne conversions up to 95.3 % are possible in the stoichiometric systems (_Both), since enough thiol is available to saturate all alkyne and methacrylate groups.

In response to the increased amount of thiol, methacrylate conversions also increase by 5.5 % to 6.6 %. This is attributed to an increased amount of thiol-ene reaction that takes place due to the excess amount of thiol.

In the reference formulation conversions tend to be lower, because domains of methacrylate still cause early vitrification and therefore limit monomer conversion. The hybrid monomers carry both moieties in one molecule, making big domains of methacrylate homopolymerization less likely. As a result, both hybrid systems exhibit higher conversions of alkyne and methacrylate.

The thiol conversions are relatively low, only ranging from 64.7 % to 78.3 %, which can be attributed to effects of sterical hindrance. Nontheless the vast majority of monomers is expected to be firmly incorporated into the polymer matrix, since the used thiol is tetrafunctional. Although not all S-H moieties react, the probability of at least one thiol moiety reacting and anchoring the molecule to the matrix is very high. In the worst case of 64.7 %

Results and discussion

conversation, the statistical likelihood of a PETMP molecule not having reacted at all is only 1.6 %.

Especially in the stoichiometric systems residual thiol is expected, since methacrylate homopolymerization consumes a certain amount of methacrylate. For every homopolymerization between two methacrylate moieties, two thiol groups are left over.

Table 3.6: Conversions of alkyne, thiol and methacrylate in ternary systems after 3 minutes of illumination and after thermal post-curing.

| Compound	Conversion after 3 min [%]			Conversion after post-curing [%]		
	Alkyne	Thiol	Methacrylate	Alkyne	Thiol	Methacrylate
UDMA_Pure			54.7			97.8
II_PETMP_UDMA_30	65.9	56.3	90.6	100.0	76.3	91.8
II_PETMP_UDMA_30_Ex	73.5	57.8	94.6	100.0	83.5	94.8
II_PETMP_UDMA_40	70.4	50.1	92.4	100.0	76.7	96.1
II_PETMP_UDMA_40_Ex	79.1	58.5	96.0	100.0	86.8	100.0
II_PETMP_UDMA_50	72.8	56.1	91.5	100.0	80.7	99.0
II_PETMP_UDMA_50_Ex	91.3	52.2	96.0	100.0	81.2	100.0
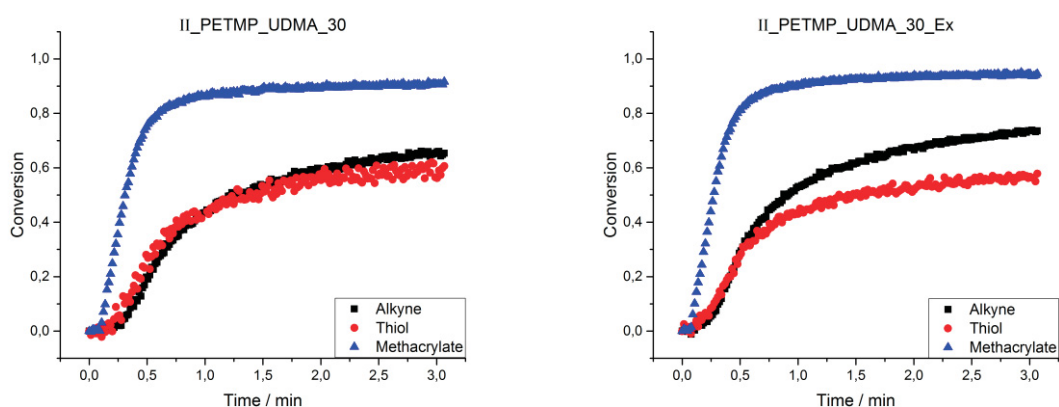
Figure 3.16: Conversions of alkyne, thiol and methacrylate groups over the course of three minutes in a non-stoichiometric (right) and a stoichiometric (left) ternary system consisting of 2-(((But-3-yn-1yloxy)ethyl methacrylate, PETMP and 30 % UDMA.

Results and discussion
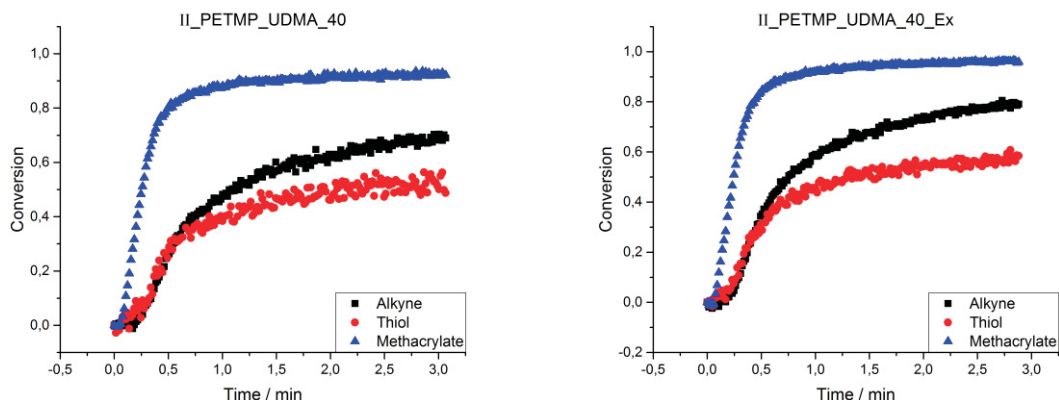
Figure 3.17: Conversions of alkyne, thiol and methacrylate groups over the course of three minutes in a non-stoichiometric (right) and a stoichiometric (left) ternary system consisting of 2-(((But-3-yn-1yloxy)ethyl methacrylate, PETMP and 40 % UDMA.
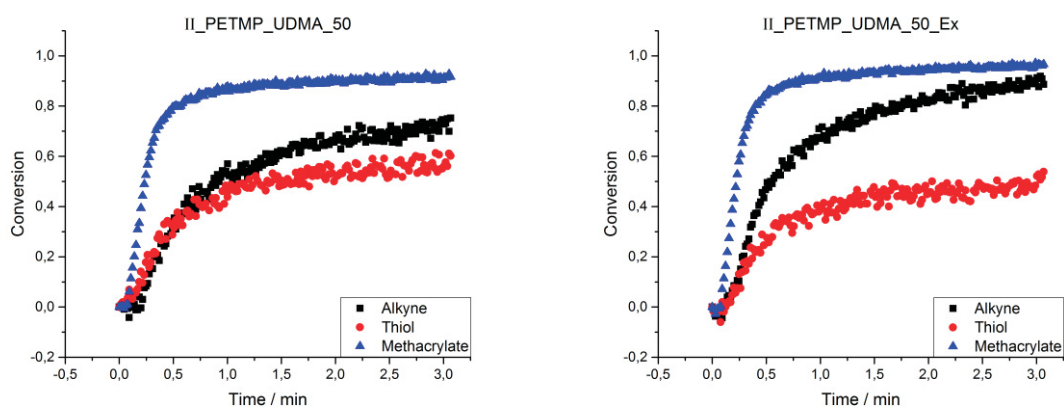
Figure 3.18: Conversions of alkyne, thiol and methacrylate groups over the course of three minutes in a non-stoichiometric (right) and a stoichiometric (left) ternary system consisting of 2-(((But-3-yn-1yloxy)ethyl methacrylate, PETMP and 50 % UDMA.

Interestingly, the systems with excess UDMA show the better conversions of alkyne and methacrylate groups, even reaching full conversions in II_PETMP_UDMA_50_Ex. Even during the illumination period of 3 minutes, the samples containing excess UDMA show higher conversions of all three functional groups, proving that the addition of moderate amounts of UDMA has no negative effect on monomer conversion.

Once more, the thiol does not fully react with the other components and seems not to be influenced by stoichiometry or overall UDMA content.

3.5 Thermo-mechanical analysis of photo-cured model formulations through dynamic mechanical analysis (DMA)

3.5.1 Comparison of a thiol-yne system to a pure acrylate

The thermo-mechanical properties of a stoichiometric compound of Butanedioldipropionate-di-malonyldibutynylester with PETMP (I_PETMP) and pure 1,4-Butanediol diacrylate (BdoAc_Pure) were investigated. The glass transition temperature (T_G) was determined as the maximum of the mechanical dissipation factor tan delta. Since possible applications for biomedical devices are targeted, the storage modulus E' was evaluated at 37 °C in order to be comparable to a physiological environment. The DMA plots are depicted in Figure 3.19 and Figure 3.20 while E' at 37 °C and the T_G are shown in Table 3.7.

1,4-Butanediol diacrylate features a storage modulus of 1400 MPa at 37 °C. Despite the slow and steady decrease of E' throughout the measurement range a maximum of tan delta could be located at 81.7°C. The absence of a well-defined T_G could be explained by the polymer's non-uniform network structure.

The thiol-yne derived compound features a E' at 37 °C of 2360 MPa, therefore surpassing the acrylate in that temperature range. In contrast to the acrylate the thiol-yne system exhibits a well-defined glass transition regime at 60.9 °C, which can be attributed to the polymer's uniform network structure.

Table 3.7: E' at 37 °C and T_G of a thiol-yne compound compared to a pure acrylate.

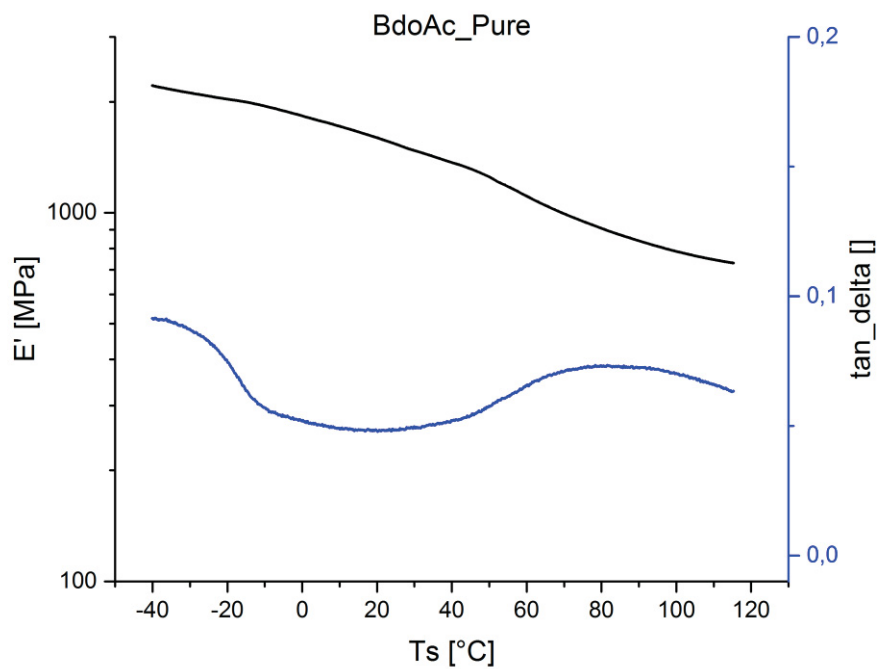| Compound	E' at 37 °C [MPa]	T_G [°C]
I_PETMP	2360	60.9
BdoAc_Pure	1400	81.7

.

Results and discussion

Figure 3.19: DMA plot of pure 1,4-Butanediol diacrylate measured at a frequency of 1 Hz from -40 °C to 120 °C.
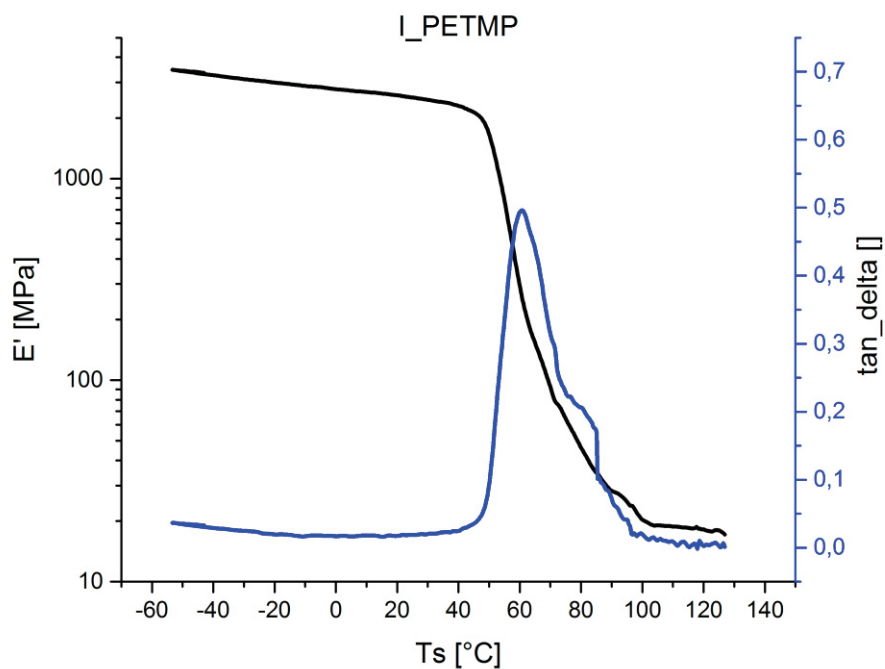

Figure 3.20: DMA plot of a stoichiometric compound of Butanedioldipropionate-di-malonyldibutynylester with PETMP measured at a frequency of 1 Hz from -50 °C to 130 °C.

3.5.2 Comparison of hybrid molecules to a reference system

The thermo-mechanical properties of non-stoichiometric compounds of 2-(((But-3-yn-1yloxy)ethyl methacrylate and 2-(((Prop-2-yn-1yloxy)ethyl methacrylate with PETMP (II_PETMP_Alkyne and III_PETMP_Alkyne) were compared to a reference system consisting of 1,4- Butanediol dipropargylcarbonate, 1,4-Butanediol dimethacrylate and PETMP (Ref_PETMP_Alkyne). The DMA plots are depicted in Figure 3.19 and Figure 3.20 while E' at 37 °C and the T_G are shown in Table 3.8.

The T_G of the hybrid systems is notably higher than the reference system (38.5 °C compared to 47.1 °C and 49.9 °C respectively). One possible explanation is the shorter C2 backbones of the hybrid monomers compared to the C4 backbones in the reference system, resulting in a higher crosslink density and a higher T_G. Although all three compounds have already started the glass transition at 37 °C, the reference system shows the lowest storage modulus (1000 MPa lower than the hybrid molecules), since the material has almost reached its T_G.

Table 3.8: E' at 37 °C and T_G of two thiol-yne-methacrylate hybrid systems compared to a thiol-yne-methacrylate reference system.

Compound	E' at 37 °C [MPa]	T_G [°C]
II_PETMP_Alkyne	1190	47.1
III_PETMP_Alkyne	1430	49.9
Ref_PETMP_Alkyne	190	38.5

Results and discussion
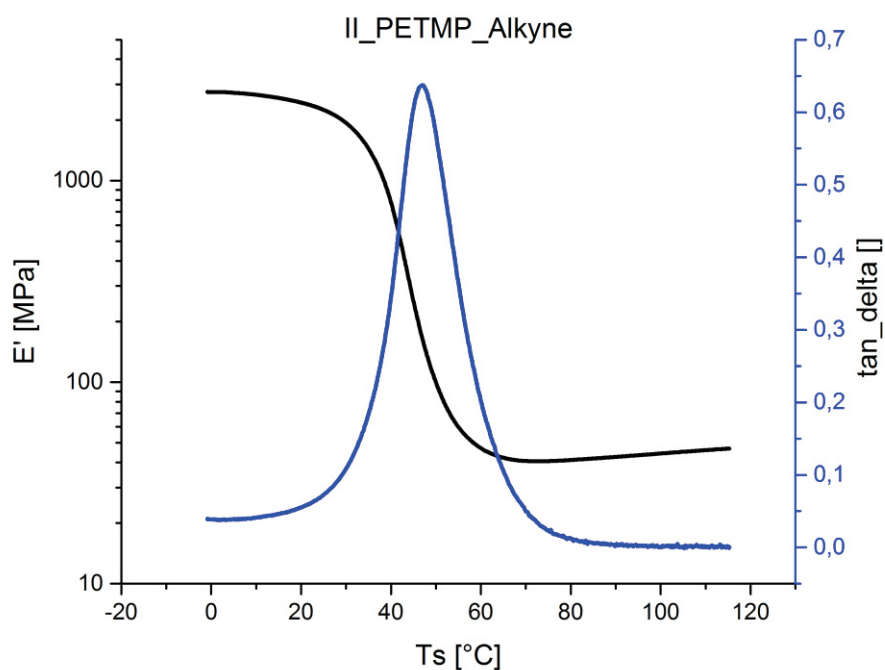
Figure 3.21: DMA plot of a non-stoichiometric compound of 2-(((But-3-yn-1yloxy)ethyl methacrylate with PETMP measured at a frequency of 1 Hz from 0 °C to 120 °C.
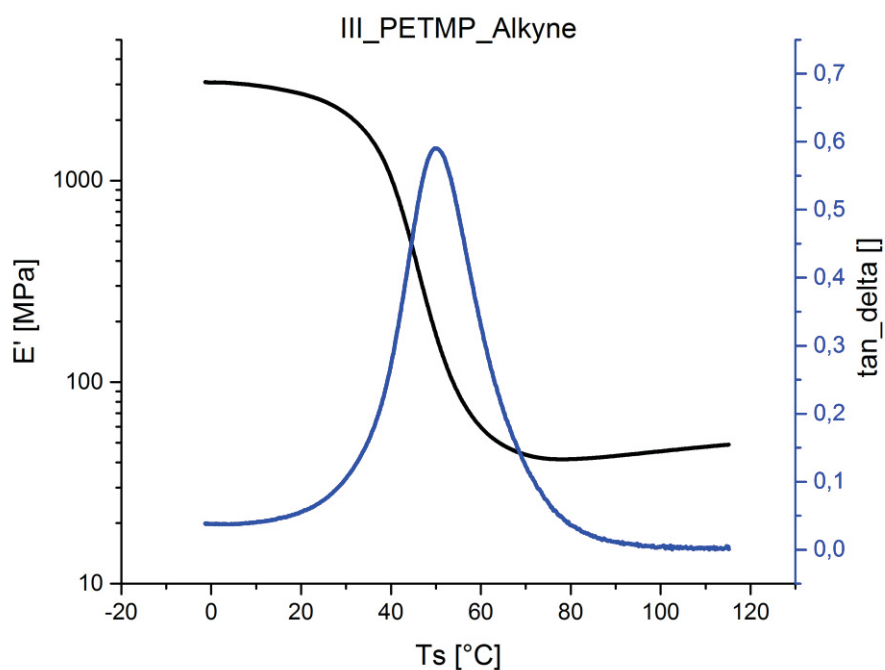

Figure 3.22: DMA plot of a non-stoichiometric compound of 2-(((Prop-2-yn-1yloxy)ethyl methacrylate with PETMP measured at a frequency of 1 Hz from 0 °C to 120 °C.
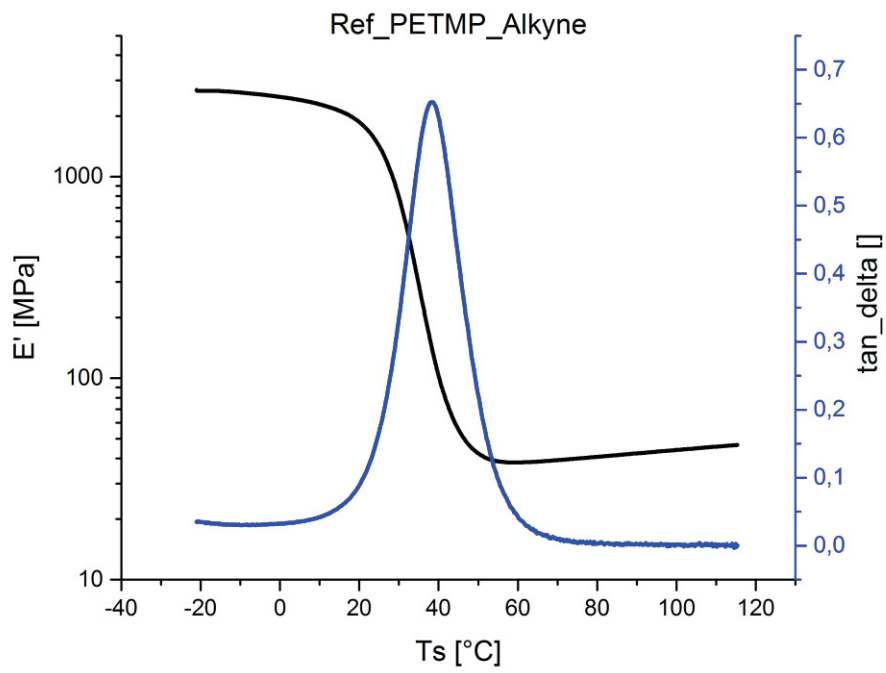
Figure 3.23: DMA plot of a non-stoichiometric compound of 1,4- Butanediol dipropargylcarbonate and 1,4-Butanediol dimethacrylate with PETMP measured at a frequency of 1 Hz from -20 °C to 120 °C.

3.6 Evaluation of polymer toughness through Crack Tip Opening Angle (CTOA) measurements

Pure 1,4-Butanediol diacrylate and a thiol-yne system composed of PETMP and Butanedioldipropionate-di-malonyldibutynylester were examinded with the CTOA criterion. Since the specimens were notched, the increase in the opening angle $\Delta\varphi$ was determined to evaluate material toughness. The results are shown in Table 3.9.

Since an early gelation point in the chain-growth polymer leads to internal stress build up, the acrylate shows brittle material behavior. Step-growth polymers on the other hand accumulate less internal stress due to a delayed gelation point and therefore exhibit a more ductile material behavior. This theory could be confirmed by the experiment's results, in which the thiol-yne compound shows a significantly larger $\Delta\varphi$ than the acrylate (8.7±2.1° versus 3.3±1.7°).

Table 3.9: CTOA of two acrylates and one thiol-yne compound.

	BdoAc_Pure	I _PETMP
	2,1	7
	5,6	11
	1,6	8
	4,4	-
	2,6	-
Average value of Δφ [°]	**3,3**	**8,7**
Standard deviation [°]	**1,7**	**2,1**

4 Conclusion & Outlook

In this contribution, possible replacements and/or supplements for commercial photo-curable (meth)acrylate resins for biomedical applications were investigated.

The novel alkyne monomer Butanedioldipropionate-di-malonyldibutynylester (I) and the two alkyne-methacrylate hybrid monomers 2-(((But-3-yn-1yloxy)ethyl methacrylate (II) and 2-(((Prop-2-yn-1-yloxy)carbonyl)oxy)ethyl methacrylate (III) could be successfully synthesized in good yields.

The reaction rates of stoichiometric and non-stoichiometric compounds containing the novel monomers and Pentaerythritol tetrakis(3-mercaptopropionate) (PETMP) were investigated through Photo-DSC and compared to pure Urethane dimethacrylate (UDMA) and a ternary thiol-yne-methacrylate reference system. In general, the stoichiometric systems exhibited faster reaction rates than non-stoichiometric systems. While I could almost reach the reaction rate of UDMA, II and III turned out to be notably slower. To address this issue, UDMA was added to systems consisting of II and PETMP. The reaction rate could be increased by up to 35.5 %, proving that the addition of UDMA to existing ternary compounds is an effective way to increase reaction rate.

The monomer conversions of various stoichiometric and non-stoichiometric compounds containing the novel monomers and PETMP were investigated by real-time FTIR-spectroscopy and compared to pure UDMA and a ternary reference system. While all other compounds required a thermal post-curing step, the thiol-yne compound containing I showed 97.4 % alkyne conversion, so that no post-curing was necessary. The compounds containing the hybrid monomers exhibited a distinct dependency on the stoichiometry of the system. While the alkyne conversions did not exceed 70 % in the non-stoichiometric systems, alkyne conversions up to 95.3 % and methacrylate conversions up to 100 % were realized in the stoichiometric compounds after post-curing. Regardless of stoichiometry, the thiol conversion did not exceed 80 % in any of the given cases.

Adding UDMA to formulations of II and PETMP was proven not to influence monomer conversions in a negative way. On the contrary, full conversions of alkyne and methacrylate and up to 86.8 % thiol conversion could be achieved by adding moderate amounts of UDMA.

1,4-Butanediol diacrylate, a thiol-yne-methacrylate reference system and compounds of I, II and III with PETMP were characterized with dynamic mechanical analysis (DMA). 1,4-Butanediol diacrylate showed a storage modulus of 1400 MPa at 37 °C and a barely visible glass transition could be observed at 81.7 °C. With a storage modulus of 2360 MPa at 37 °C the thiol-yne system containing I showed the highest storage modulus of the three novel monomers, even surpassing the acrylate. A well-defined glass transition could be

observed at 60.9 °C. The ternary reference system exhibited a lower T_G (38.5 °C) than the compounds containing the hybrid monomers II (47.1 °C) and III (49.9 °C). As a result, E' at 37 °C of both hybrid monomers exceeded the reference system at least by 1000 MPa.

A stoichiometric compound of I with PETMP was characterized with Crack Tip Opening Angle (CTOA) measurements and compared with pure 1,4-Butanediol diacrylate. The acrylate features a chain-growth mechanism, resulting in increased internal stress and overall brittle material behavior. However, the thiol-yne system containing I features a step-growth mechanism, which leads to less internal stress due to its delayed gelation point. As a result, the CTOA of the thiol-yne system (8.7±2.1°) was larger than in the acrylate system (3.3±1.7°).

Future studies should work towards determining an optimal ratio between all monomers in ternary systems, providing even better monomer conversions and crosslink density. In order to improve the E' and T_G in thiol-yne-methacrylate systems novel monomers with more rigid backbone structures should be explored. In addition, more detailed characterization of material toughness should be conducted.

5 Experimental

5.1 Synthesis

5.1.1 Synthesis of Malonyldibutynylester (Ia)
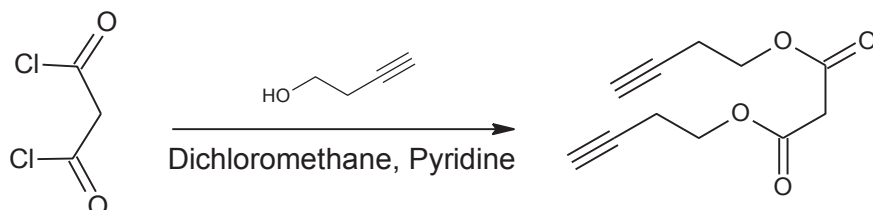
10.0 g of Malonyl chloride (71.0 mmol, 1.0 eq) were dissolved in 40.0 ml Dichloromethane and cooled to 0 °C. 11.6 ml of Pyridine (11.8 g, 149.0 mmol, 2.1 eq) were added to the mixture. In a final step, 11.4 g of 3-Butyn-1-ol (163.2 mmol, 2.3 eq) were added dropwise before allowing the mixture to stir for 8 h at room temperature. After the solvent was evaporated, the crude product was purified by distillation, yielding Ia as a transparent colorless liquid.

Yield: 12.0 g (81.5 %)

^{1}H-NMR: (δ, 400 MHz, 25 °C, CDCl$_3$):

4.30 (t, J = 7.1 Hz, 4H, CH2), 3.14 (s, 2H, CH2), 2.75 (t, J = 6.7 Hz, 2H, CH), 2.16 (m, 4H, CH2).

^{13}C-NMR: (δ, 400 MHz, 25 °C, CDCl$_3$):

161.14 (2C, C=O); 80.61 (2C, C); 70.47 (2C, CH); 60.95 (2C, CH2); 39.17 (1C, CH2); 21.01 (2C, CH2) ppm.

Experimental

5.1.2 Synthesis of Butanedioldipropionate-di-malonyldibutynylester (I)
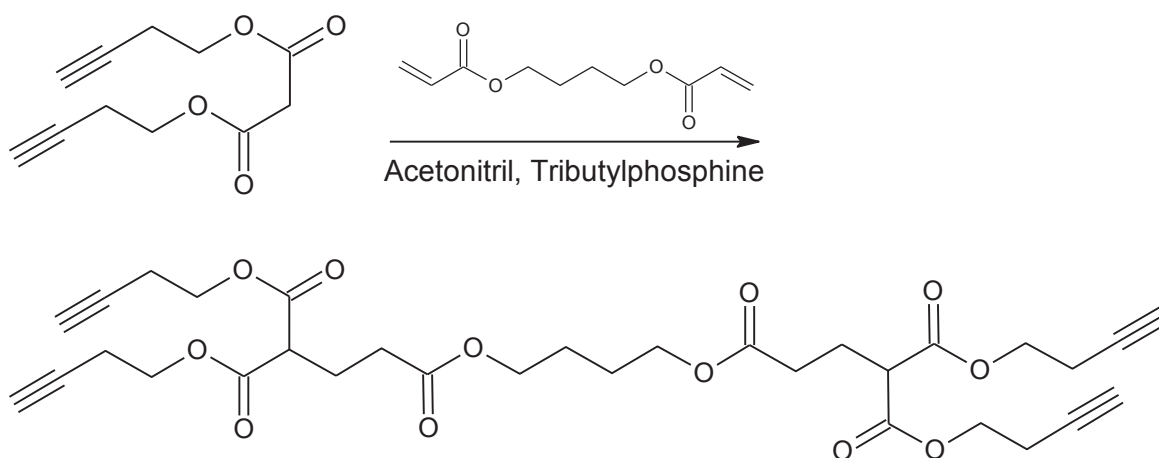
1.0 g 1,4-Butanediol diacrylate (5.1 mmol, 1 eq) was added dropwise into a solution of 21.0 g Malonyldibutynylester (101.0 mmol, 20 eq) and 0.1 g Tributylphosphine (0.5 mmol, 0.1 eq) in 140 ml Acetonitrile. The mixture was heated to 50 °C and was allowed to stir for 10 h. The solvent was evaporated under reduced pressure and the crude product was dissolved in 50 ml Dichloromethane before being washed with HCl (5 %), saturated $NaHCO_3$, water and dried over Na_2SO_4. After removing the solvent under reduced pressure the residual crude product was purified by column chromatography (250 g Silica gel, Cyclohexane:Ethyl acetate = 2:1), yielding a colorless transparent liquid.

Yield: 2.1 g (67.0 %)

^{1}H-NMR: (δ, 400 MHz, 25 °C, $CDCl_3$):

4.29 (t, J = 7.0 Hz, 8H, CH_2), 4.20 (t, J = 7.2 Hz, 4H, CH_2), 3.27 (m, 2H, CH), 2.91 (t, J = 6.9 Hz, 4H, CH), 2.36 (m, 16H, CH_2), 1.51 (m, 4H, CH_2).

^{13}C-NMR: (δ, 400 MHz, 25 °C, $CDCl_3$):

172.49 (2C, C=O); 164.66 (4C, C=O); 81.78 (4C, C); 70.15 (4C, CH); 65.08 (2C, CH_2); 62.76 (4C, CH_2); 50.98 (2C, CH); 30.41 (2C, CH_2); 27.42 (2C, CH_2); 22.73 (2C, CH_2); 22.46 (4C, CH_2) ppm.

Experimental

5.1.3 Synthesis of But-3-yn-1-yl-1H-imidazole-1-carboxylate (IIa)
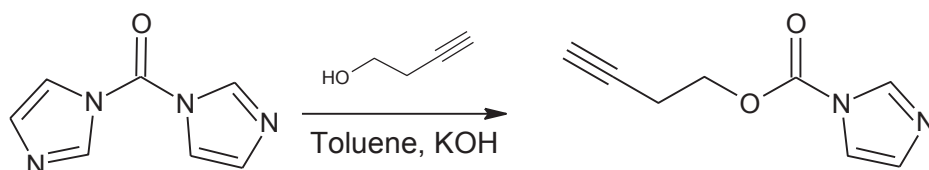
22.2 g of 1,1′-Carbonyldiimidazole (CDI) (137.0 mmol, 1.2 eq) and 30 mg (0.5 mmol) KOH were suspended in 160 ml of Toluene. 8.0 g of 3-Butyn-1-ol (114.1 mmol, 1.0 eq) were added dropwise, which lead to a dissolution of the solid reactants. The mixture was allowed to stir at 60 °C for 12 h. Afterwards the solvent was evaporated under reduced pressure and the white solid was dissolved in 30 ml of Dichloromethane. The crude product was then washed with water. The organic layer was dried over Na_2SO_4 and evaporated under reduced pressure. The procedure yielded IIa as a white solid which could be processed without further purification.

**Yield:** 17.5 g (93.3 %)

^{1}H-NMR: (δ, 400 MHz, 25 °C, CDCl$_3$):

8.08 (s, 1H, AR), 7.40 (d, J = 7.8 Hz, 1H, AR), 6.99 (d, J = 7.8 Hz, 1H, AR), 4.92 (d, J = 2.5 Hz, 2H, CH2), 2.61 (t, J = 2.5 Hz, 1H, CH), 1.36 (t, J = 7.1 Hz, 2H, CH2) ppm.

^{13}C-NMR: (δ, 400 MHz, 25 °C, CDCl$_3$):

150.20 (1C, C=O); 136.81 (1C, AR); 130.84 (1C, AR); 117.66 (1C, AR); 81.49 (1C, C); 69.70 (1C, CH); 60.27 (1C, CH2); 21.71 (C, CH2) ppm.

Experimental

5.1.4 Synthesis of 2-(((But-3-yn-1yloxy)ethyl methacrylate (II)
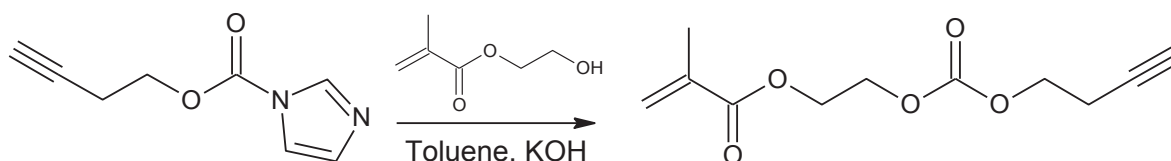
14.0 g of But-3-yn-1-yl 1,4-imidazole-1-carboxylate (85.3 mmol, 1.3 eq) were dissolved in 140 ml Toluene before 30 mg (0.5 mmol) KOH were added. 8.5 g 2-Hydroxyethyl methacrylate (HEMA) (65.6 mmol, 1.0 eq) were then added dropwise before leaving the mixture to stir for 10 h at 60 °C. The solvent was evaporated under reduced pressure and the crude product subsequently dissolved in Dichloromethane. The mixture was washed with water before the organic layer was separated and dried over Na_2SO_4. The solvent was removed under reduced pressure before the crude product could be purified by column chromatography (250 g Silica gel, Cyclohexane:Ethyl acetate = 4:1), yielding a colorless transparent liquid.

Yield: 10.6 g (71.2 %)

^{1}H-NMR: (δ, 400 MHz, 25 °C, CDCl$_3$):

6.10 (s, 1H, CH2), 5.55 (s, 1H, CH2), 4.34 (d, J = 2.3 Hz, 4H, CH2), 4.06 (m, 1H, CH), 1.91 (d, J = 4.6 Hz, 2H, CH2), 1.67 (m, 2H, CH2), 0.92 (s, 3H, CH3) ppm.

^{13}C-NMR: (δ, 400 MHz, 25 °C, CDCl$_3$):

167.23 (1C, C=O); 155.51 (1C, C=O); 136.02 (1C, C); 125.21 (1C, C=C); 81.41 (1C, C), 69.92 (1C, C), 66.84 (2C, CH2); 62.42 (2C, CH2); 18.0 (1C, CH3) ppm.

5.1.5 Synthesis of Prop-2-yn-1-yl-1H-imidazole-1-carboxylate (VIa)
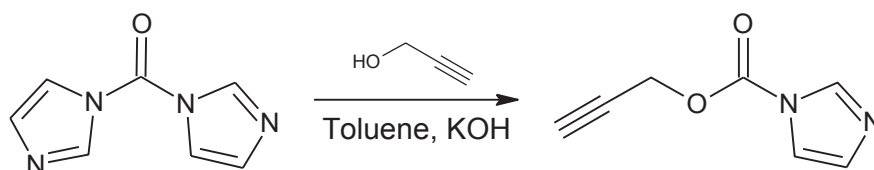
27.8 g CDI (1.2 eq, 171.2 mmol) and 30 mg (0.5 mmol) KOH were suspended in 160 ml of Toluene. Subsequently, 8.0 g Propargyl alcohol (142.7 mmol, 1.0 eq) were added dropwise, which lead to a dissolution of the solid reactants. The mixture was left to stir at 60 °C for 12 h. Afterwards the solvent was evaporated under reduced pressure and the white solid was dissolved in 30 ml of Dichloromethane. The crude product was the washed with water before the organic layer was dried over Na_2SO_4. The solvent was removed under reduced pressure and the product IIIa was obtained as a white solid which could be processed without further purification.

Yield: 21.2 g (90.5 %)

^{1}H-NMR: (δ, 400 MHz, 25 °C, CDCl$_3$):

8.11 (s, 1H, AR), 7.40 (d, J = 7.4 Hz, 1H, AR), 7.03 (d, J = 7.8 Hz, 1H, AR), 4.95 (d, J = 2.5 Hz, 2H, CH2), 2.61 (t, J = 2.5 Hz, 1H, CH) ppm.

^{13}C-NMR: (δ, 400 MHz, 25 °C, CDCl$_3$):

147.98 (1C, C=O); 137.13 (1C, AR); 130.81 (1C, AR); 117.10 (1C, AR); 77.05 (1C, C); 75.76 (1C, CH); 55.32 (1C, CH2).

Experimental

5.1.6 Synthesis of 2-(((Prop-2-yn-1-yloxy)carbonyl)oxy)ethyl methacrylate (III)
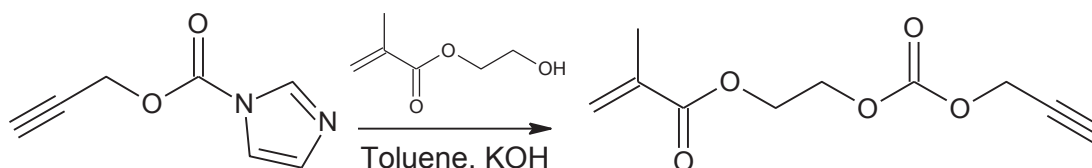
14.5 g of Prop-2-yn-1-yl-1H-imidazole-1-carboxylate (88.3 mmol, 1.3 eq) were dissolved in 140 ml Toluene before 30 mg (0.5 mmol) KOH were added. 8.6 g HEMA (66.4 mmol, 1.0 eq) were added dropwise before allowing the mixture to stir for 10 h at 60 °C. The solvent was removed under reduced pressure and the crude product subsequently dissolved in Dichloromethane. The mixture was washed with water before the organic layer was separated and dried over Na_2SO_4. The solvent was removed under reduced pressure before the crude product could be purified by column chromatography (250 g Silica gel, Cyclohexane:Ethyl acetate = 4:1), yielding a colorless transparent liquid.

Yield: 9.1 g (60.7 %)

^{1}H-NMR: (δ, 400 MHz, 25 °C, CDCl$_3$):

6.09 (s, 1H, CH2), 5.56 (s, 1H, CH2), 4.70 (d, J = 2.1 Hz, 4H, CH2), 4.35 (d, J = 4.1 Hz, 2H, CH2), 2,52 (m, 1H, CH), 1.90 (s, 3H, CH3) ppm.

^{13}C-NMR: (δ, 400 MHz, 25 °C, CDCl$_3$):

157.46 (1C, C=O); 141.42 (1C, C=O); 124.12 (1C, C); 112.98 (1C, C=C); 80.02 (1C, C), 74.15 (1C, C), 67.15 (2C, CH2); 61.84 (1C, CH2); 18.0 (1C, CH3) ppm.

5.2 **Methods and equipment**

5.2.1 ^{1}H-NMR and ^{13}C-NMR spectroscopy

^{1}H-NMR and ^{13}C-NMR spectroscopy was performed on a Varian 400-NMR spectrometer operating at 399.66 MHz and 100 MHz respectively. A relaxation delay of 10 s and a 45° pulse were used for acquisition of the ^{1}H-NMR spectra. In agreement with values given in the literature [64] peaks of residual solvent were used to reference the NMR spectra.

5.2.2 Thin-layer chromatography (TLC)

Reactions were monitored by TLC (Silica gel 60 F254 on aluminum, Merck). Detection was conducted by UV-light (254 nm and 365 nm for fluorescent/phosphorescent compounds), by staining with Potassium permanganate (2 % in H_2O dest.) and iodine absorption.

5.2.3 Crack Tip Opening Angle (CTOA)

The measurement was conducted in three-point bending mode with a traverse speed of 1 mm/min and a support distance of 40 mm. The specimens were notched with a razor-sliding blade with a maximum thickness of 200 µm. The crack propagation was monitored with a high-speed camera at 250 Hz, whereas the difference of the CTOA between the first frame (first contact with the peen) and the last frame (failure of test specimen) was determined as $\Delta\varphi$ and used to qualitatively compare material behavior.

5.2.4 Fourier transformed infrared spectroscopy (FTIR)

FTIR measurements were conducted on a VERTEX 70 (Bruker, Billerica, USA) in reflection mode with the unit A513. 1 µL of the resin of investigation was placed in between two CaF_2 windows (8 mm diameter, 1 mm thickness) and illuminated with an Omnicure s1000 (Lumen Dynamics, Mississauga, USA) at 20 % intensitiy with 9 cm gap between the sample and light guide (P = 22 mW*cm^{-2} at the sample surface). After illumination the specimens were also post-cured thermally at 100 °C for 16 hours. The corresponding monomers were mixed with 3 wt% of the photoinitiator Ethyl (2,4,6-trimethylbenzoyl) phenylphosphinate (Irgacure TPO-L) and a stoichiometric amount of Pentaerythritol tetra(3-mercaptopropionate) (PETMP).

Experimental

5.2.5 Photo differential scanning calorimetry (Photo-DSC)

The Photo-DSC experiments were performed on a NETZSCH Photo-DSC 204 F1 Phoenix. All measurements were conducted at 50 °C in aluminum crucibles under nitrogen flow (20 mL*min^{-1}). An Omnicure s2000 UV-Lamp was used as light source at 1 W*cm^{-2} resulting in an intensity of 80 mW cm^{-2} at the surface of the sample (range of wavelength was 250 - 445 nm). For the determination of the reaction enthalpy and t_{max}, the samples were illuminated twice for 10 min each with an idle time of 2 min in between (sample quantity: 8 ± 0.05 mg resin, containing 3 wt% of Irgacure TPO-L and stoichiometric amounts of PETMP). For the analysis, the second run was subtracted from the first one to obtain the reaction enthalpy curve.

5.2.6 Sample preparation

For the determination of the thermo-mechanical properties and toughness properties of the photopolymers, sample specimens with 1 x 4 x 25 mm^3 (DMA) and 2 x 8 x 50 mm^3

(CTOA) rectangular dimensions were fabricated. The resins contained 3 wt% of the photoinitiator Irgacure TPO-L. The resin samples were photocured by a Lighthammer 6 (Fusion UV Systems) with a Hg bulb (5 passes each side with a belt speed of 8 m/min at 25 % light intensity, then 5 passes each side with a belt speed of 4 m/min at 25, 40, 50 % light intensity and then 10 passes each side with a belt speed of 4 m/min at 60 % light intensity). After illumination the specimens were also post-cured thermally at 100 °C for 16 hours.

5.2.7 Dynamic mechanical thermal analysis (DMA)

The thermo-mechanical properties were measured in tension mode using a DMA/SDTA 861 (Mettler Toledo) with a heating rate of 2 K*min^{-1} in the temperature range from -50 to 130 °C. The operating frequency was determined at 1 Hz. The glass transition temperature was determined at the maximum of tan delta.

Experimental

5.2.8 Materials

Table 5.1: List of chemicals.

Substance	producer	grade
Acetonitrile	Sigma-Aldrich	≥ 99.5 %
1,4-Butanediol diacrylate	Sigma-Aldrich	90 %
3-Butyn-1-ol	Sigma-Aldrich	97 %
1,1'-Carbonyldiimidazole (CDI)	Sigma-Aldrich	reagent grade
Cyclohexane	VWR Chemicals	100 %
Dichloromethane	VWR Chemicals	≥ 98 %
Ethyl acetate	VWR Chemicals	99.9 %
Ethyl (2,4,6-trimethylbenzoyl) phenylphosphinate (Irgacure TPO-L)	BASF	n/a
Hydrochloric acid	Roth	37 %
Hydroxyethyl methacrylate (HEMA)	Sigma-Aldrich	97 %
Malonyl chloride	Sigma-Aldrich	97 %
Pentaerythritol tetraacrylate	Sigma-Aldrich	n/a
Pentaerythritol tetra(3-mercaptopropionate) (PETMP)	Bruno Bock Chemische Fabrik GmbH & Co. KG	n/a
2-Propyn-1-ol	Sigma-Aldrich	99 %
Pyridine	Sigma-Aldrich	anhydrous, 99.8 %
Sodium hydrogencarbonate	Fluka	≥ 99 %
Sodium hydroxide	Fluka	purum, ≥ 97 %
Sodium sulfate	Merck	anhydrous, p.a.
Toluene	Roth	p.a.
Tributylphosphine	Sigma-Aldrich	97 %

1,4-Butanediol diacrylate was purified by distillation under reduced pressure before usage. All other reagents were used without further purification.

6 APPENDIX

6.1 List of Abbreviations

Austrian Science fund	FWF
1,1′-Carbonyldiimidazole	CDI
Christian Doppler Laboratory	CDL
Computer-aided design	CAD
Computer tomography	CT
Crack tip opening angle	CTOA
Deoxyribonucleic acid	DNA
N,N′-Dicyclohexylcarbodiimide	DCC
Digital light projector	DLP
4-(Dimethylamino)pyridine	DMAP
Diurethane dimethacrylate	UDMA
Dynamic mechanical analysis	DMA
Glass transition temperature	T_g
Hydroxy ethyl methacrylate	HEMA
Magnetic resonance imaging	MRI
Nuclear magnetic resonance	NMR
Pentaerythritol tetrakis(3-mercaptopropionate)	PETMP
Real-time Fourier transform infrared spectroscopy	Real-time FTIR
Photo-differential scanning calorimetry	Photo-DSC
Ultraviolet	UV

6.2 **List of figures**

6.3   **List of Tables**

7 References

[1] F. Valente, G. Schiroli und A. Sbrenna, *Int. J. Oral Maxillofac. Implants,* 2009, 24, 234-242.

[2] J. Banks, *IEEE Pulse,* 2013, 4, 22-26.

[3] N. J. Mankovich, D. Samson, W. Pratt, D.Lew und J. Beumer, *Otolaryngol. Clin. North Am.,* 1994, 27, 875-889.

[4] A. Dawood, B. M. Marti, V. Sauret-Jackson und A. Darwood, *Br. Dent. J.,* 2015, 219, 521-529.

[5] A. Curodeau, E. Sachs und S. Caldarise, *J. Biomed. Mater. Res.,* 2000, 53, 525-535.

[6] B. Husár, C. Heller, M. Schwentenwein, A. Mautner, F. Varga, T. Koch, J. Stampfl und R. Liska, *J. Polym. Sci. A Polym. Chem.,* 2011, 49, 4927-4934.

[7] A. Woesz, M. Rumpler, J. Stampfl, F. Varga, N. Fratzl-Zelman, P. Roschner, K. Klaushofer und P. Fratzl, *Mater. Sci. Eng. C,* 2005, 25, 181-186.

[8] L. E. Murr, E. Martinez, K. N. Amato, S. M. Gaytan, J. Hernandez, D. A. Ramirez, P. W. Shindo, F. Medina und R. B. Wicker, *J. Mater. Techn.,* 2012, 1, 42-54.

[9] D. L. Bourell, H. L. Marcus, J. W. Barlow und J. J. Beaman, *Int. J. Powder Metall,* 1992, 28, 369-381.

[10] P. H. Warnke, H. Seitz, F. Warnke, S. T. Becker, S. Sivananthan, R. Sherry, Q. Liu, J. Wiltfang und T. Douglas, *J. Biomed. Mater. Res. B Appl. Biomater.,* 2010, 93, 212-217.

[11] A. Zocca, P. Colombo, C. M. Gomes, J. Günster und D. J. Green, *J. Am. Ceram. Soc.,* 2015, 98,1983-2001.

[12] R. Liska, M. Schuster, R. Inführ, C. Turecek, C. Fritscher, B. Seidl, V. Schmidt, L. Kuna, A. Haase, F. Varga, H. Lichtenegger und J. Stampfl, *J. Coat. Technol. Res.,* 2007, 4, 505-510.

[13] B. Wendel, D. Rietzel, F. Kühnlein, R. Feulner, G. Hülder und E. Schmachtenberg, *Macromol. Mater. Eng.,* 2008, 293, 799-809.

[14] R. D. Goodridge, C. J. Tuck und R. Hague, *Prog. Mater. Sci.,* 2012, 57, 229-267.

References

[15] H. N. Chia und B. M. Wu, *J. Biol. Eng.,* 2015, 9, 4.

[16] M. Schuster, C. Turecek, G. Weigel, R. Saf, J. Stampfl, F. Varga und R. Liska, *J. Polym. Sci. A Polym. Chem.,* 2009, 47, 7078-7089.

[17] S. C. Ligon-Auer, M. Schwentenwein, C. Gorsche, J. Stampfl und R. Liska, *Poly. Chem.,* 2016, 7, 257-286.

[18] C. Gorsche, K. Seidler, P. Knaack, P. Dorfinger, T. Koch, J. Stampfl, N. Moszner und R. Liska, *Polym. Chem.,* 2016, 7, 2009-2014.

[19] D. Karalekas und A. Aggelopoulos, *J. Mater. Process. Tech.,* 2003, 136, 146-150.

[20] L. S. Andrews und J. J. Clary, *J. Toxikol. Environ. Health,* 1986, 19, 149-164.

[21] M. Friedman, J. F. Cavins und J. S. Wall, *J. Am. Chem. Soc.,* 1965, 87, 3672-3682.

[22] I. Vroman und L. Tighzert, *Materials,* 2009, 2, 307-344.

[23] A. Mautner, X. Qin, G. Kapeller, G. Russmüller, T. Koch, J. Stampfl und R. Liska, *Macromol. Rapid Commun,* 2012, 33, 2046-2052.

[24] J. C. Middleton und A. J. Tipton, *Biomaterials,* 2000, 21, 2335-2346.

[25] A. Oesterreicher, S. Ayalur-Karunakaran, A. Moser, F. H. Mostegel, M. Edler, P. Kaschnitz, G. Pinter, G. Trimmel, S. Schlögl und T. Griesser, *J. Polym. Sci. A,* 2016, 54, 3484-3495.

[26] A. Oesterreicher, J. Wiener, M. Roth, A. Moser, R. Gmeiner, M. Edler, G. Pinter und T. Griesser, *Polym. Chem.,* 2016, 7, 5169-5180.

[27] A. Oesterreicher, C. Gorsche, S. Ayalur-Karunakaran, A. Moser, M. Edler, G. Pinter, S. Schlögl, R. Liska und T. Griesser, *Macromol. Rapid Commun,* 2016, 37, 1701-1706.

[28] M. Roth, A. Oesterreicher, F. H. Mostegel, A. Moser, G. Pinter, M. Edler, R. Piock und T. Griesser, *J. Polym. Sci. Part A: Polym. Chem.,* 2016, 54, 418-424.

[29] A. F. Jacobine, *Elsevier,* 1993, 7, 219-268.

[30] C. N. Bowman und C. J. Kloxin, *AIChE J.,* 2008, 54, 2775-2795.

[31] C. Hoyle, T. Y. Lee und T. Roper, *Polym. Sci., Polym. Chem.,* 2004, 42, 5301-5338.

[32] L. H. Hung, R. Lin und A. P. Lee, *Lab Chip,* 2008, 8, 983-987.

References

[33] B. T. Good, S. Reddy, R. H. Davis und C. N. Bowman, *Sens. Actuators B,* 2007, 120, 473-480.

[34] E. W. Moran, A. L. Briseno, S. Loser und K. R. Carter, *Chem. Mater.,* 2008, 20, 4595-4601.

[35] C. N. Bowman and N. A. Peppas, *Macromolecules,* 1991, 24, 1914-1920.

[36] H. Lu, J. W. Stansbury and C. N. Bowman, *Dent. Mater.,* 2004, 20, 979-986.

[37] J. P. Fouassier und J. F. Rabek, *Elsevier Science Publishers Ltd.: Essex,* 1993, Vol. I, pp 7-9.

[38] M. Roper, T. Y. Lee, C. A. Guymon und C. E. Hoyle, *Macromolecules,* 2005, 38, 10109-10116.

[39] L. J. Gou, B. Opheim, C. N. Coretsopolous und A. B. Scranton, *Chem. Eng. Commun.,* 2006, 193, 620-627.

[40] H. C. Kolb, M. G. Finn und K. B. Sharpless, *Angew. Chem,* 2001, 113, 2056-2075.

[41] H. C. Kolb, M. G. Finn und K. B. Sharpless, *Angew. Chem. Int. Ed.,* 2001, 40, 2004-2021.

[42] C. Hoyle und C. N.Bowman, *Angew. Chem.,* 2010, 122, 1584-1617.

[43] N. B. Cramer und C. N. Bowman, *J. Polym. Sci., Polym. Chem. ,* 2001, 39, 3311-3319.

[44] H. Lu, J. A. Carioscia, J. W. Stansbury und C. N. Bowman, *Dent. Mater.,* 2005, 21, 1129-1136.

[45] M. Patel, M. Braden und K. W. M. Davy, *Biomaterials,* 1987, 8, 53-56.

[46] B. D. Mather, K. Viswanathan, K. V. Miller und T. E. Long, *Prog. Polym. Sci.,* 2006, 31, 487-531.

[47] S. Reinelt, M. Tabatabai, N. Moszner, U. K. Fischer, A. Utterodt und H. Ritter, *Macromol. Chem. Phys.,* 2014, 215, 1415-1425.

[48] S. Parker, R. Reit, H. Abitz, G. Ellson, K. Yang, B. Lund und W. E. Voit, *Macromol. Rapid Commun,* 2016, 37, 1027-1032.

[49] M. Podgórski, E. Becka, S. Chatani, M. Claudino und C. N. Bowman, *Polym. Chem.,* 2015, 6, 2234-2240.

References

[50] J. A. Carioscia, L. Scheidewind, C. O'Brien, R. Ely, C. Feeser, N. Cramer und C. N. Bowman, *J. Polym. Sci. A Polym. Chem.,* 2007, 45, 5686-5696.

[51] B. D. Fairbanks, T. F. Scott, C. J. Kloxin, K. S. Anseth und C. N. Bowman, *Macromolecules,* 2009, 42, 211-217.

[52] B. D. Fairbanks, E. A. Sims, K. S. Anseth und C. N. Bowman, *Macromolecules, ,* 2010, 43, 4113-4119.

[53] J. W. Chan, J. Chin, C. E. Hoyle, C. N. Bowman und A. B. Lowe, *Macromolecules,* 2010, 43, 4937-4942.

[54] J. W. Chan, H. Zhou, C. E. Hoyle und A. B. Lowe, *Chem. Mater.,* 2009, 21, 1579-1585.

[55] S. K. Reddy, N. B. Cramer und C. N. Bowman, *Macromolecules,* 2006, 39, 3681-3687.

[56] T. Y. Lee, J. Carioscia, Z. Smith und C. N. Bowman, *Macromolecules,* 2007, 40, 1473-1479.

[57] N. Cramer, C. L. Couch, K. M. Schreck, J. A. Carioscia, J. E. Boulden, J. Stansbury und C. N. Bowman, *Dent. Mater.,* 2010, 26, 21-28.

[58] S.Ye, N. B. Cramer, I. R. Smith, K. R. Voigt und C. N. Bowman, *Macromolecules,* 2011, 44, 9084-9090.

[59] [Online]. Available: https://www.netzsch-thermal-analysis.com/en/products-solutions/differential-scanning-calorimetry/dsc-214-polyma/. [Zugriff am 31 05 2017].

[60] X. K. Zhu und J. A. Joyce, *Engng. Fract. Mech.,* 2012, 85, 1-46.

[61] B. V. Gross, J. L. Erkal, S. Y. Lockwood, C. Chan und D. M. Spencer, *Anal. Chem.,* 2014, 86,3240-3253.

[62] C. Hull, „Apparatus for production of three-dimensional objects by stereolithography". Patent US 4575330 A, 1986.

[63] F. P. W. Melchels, J. Feijen und D. W. Grijpma, *Biomaterials,* 2010, 31, 6121-6130.

[64] H. E. Gottlieb, V. Kotlyar und A. J. Nudelman, *Org. Chem ,* 1997, 62, 7512-7515.

[65] V. S. Khire, Y. Yi, N. A. Clark und C. N. Bowman, *Adv. Mater.,* 2008, 20, 3308-3313.

[66] S. K. Reddy, R. P. Sebra, K. S. Anseth und C. N. Bowman, *J. Polym. Sci. Part A,* 2005, 43, 2134-2144.

References

[67] E. C. Hagberg, M. Malkoch, Y. B. Ling, C. J. Hawker und K. R. Carter, *Nano Lett.,* 2007, 7, 233-237.

[68] Z. Hordyjewicz-Baran, L. C. You, B. Smarsly, R. Sigel und H. Schlaad, *Macromolecules,* 2007, 40, 3901-3903.

[69] J. Justynska, Z. Hordyjewicz und H. Schlaad, *Polymer,* 2005, 46, 12057-12064.

[70] D. H. Lim, H. S. Do, H. J. Kim, J. S. Bang und G. H. Yoon, *J. Adhes. Sci. Technol.,* 2007, 21, 589-603.

[71] A. Taguet, B. Ameduri und B. Boutevin, *Crosslinking in Materials Science, Vol. 184, Springer, Berlin,* 2005, 127-211.

[72] [Online]. Available: http://www.pcimag.com/articles/85843-the-use-of-specialty-acrylic-esters-in-cure-in-place-coating-technology. [Accessed 06 03 2017].

[73] [Online]. Available: https://www.researchgate.net/figure/227997470_fig10_Figure-1-Scheme1-Generalized-radical-thiol-ene-click-reaction-possible-reaction. [Zugriff am 06 03 2017].

[74] J. P. Fouassier, Photoinitiation, Photopolymerization and Photocuring: Fundamentals and Applications, New York: Hanser Publisher, 1995.

[75] A. B. Scranton, C. N. Bowman und R. W. Pfeiffer, Photopolymerization: Fundamentals and Applications, Washington, DC: American Chemical Soc, 1997, vol. 673.

[76] N. S. Allen, Photopolymerization and Photoimaging Science and Technology, London, 1st edn.: Elsevier Applied Science, 1989.